www.sciencemag.org/content/343/6174/1002/suppl/DC1

Supplementary Materials for

Promoter-Bound Trinucleotide Repeat mRNA Drives Epigenetic Silencing in Fragile X Syndrome

Dilek Colak, Nikica Zaninovic, Michael S. Cohen, Zev Rosenwaks, Wang-Yong Yang, Jeannine Gerhardt, Matthew D. Disney, Samie R. Jaffrey*

*Corresponding author. E-mail: srj2003@med.cornell.edu

Published 28 February 2014, *Science* **343**, 1002 (2014)
DOI: 10.1126/science.1245831

This PDF file includes

MATERIALS AND METHODS

Generation and Teratoma Formation of hESC Lines

We recently described the Fragile X Syndrome (FXS) human embryonic stem cell (hESC) lines WCMC-37 and SI-214 used in this study (*8*). SI-214 was purchased from Stemride International Limited (Chicago, IL). Control (WCMC-7) and *FMR1* premutation (WCMC-5 and WCMC-13) hESC lines were generated from in vitro fertilization (IVF)-derived embryos during preimplantation genetic diagnosis (PGD). These embryos were tested for the presence of an expanded CGG allele, and embryos that showed evidence of an elongated *FMR1* allele were not used for in vitro fertilization. In accordance with the Weill Cornell Embryonic Stem Cell Research Oversight Committee (ESCRO) these embryos were donated for the purpose of creating hESC lines. The use of these IVF-derived embryos for the generation of hESC was approved by Weill Cornell Medical College Institutional review board (Protocol No.0502007737). The WCMC-37 hESC line was recently approved as an NIH Embryonic Stem Cell Registry line (NIH registration number 211, NIH Approval Number: NIHhESC-13-0211). Requests for WCMC hESC lines should be directed to N.Z. (nizanin@med.cornell.edu) and Z.R. (zrosenw@med.cornell.edu). Requests for other hESC lines should be directed to S.R.J. (srj2003@med.cornell.edu).

Embryos were cultured to the blastocyst stage. hESC lines were derived by laser inner cell mass (ICM) dissection of the blastocyst on day 6 as described previously (*28*). Isolated clumps of ICM cells were cultured on mouse embryonic fibroblasts (MEF, GlobalStem). Outgrowth-containing cells were manually cut and propagated, resulting in a stable culture of undifferentiated hESC. All hESC lines were fully characterized by stem cell markers in vitro and teratoma formation in vivo. hESCs were injected in non-obese diabetic/severe combined immunodeficient (NOD-SCID) mice that do not reject human cells. 1-5 million hESC cells were injected together with BD Matrigel (1:1, total volume 0.5 ml). After approximately two months, mice were sacrificed and the teratoma tissues were carefully dissected from the host tissues, washed in PBS and fixed overnight in 4% paraformaldehyde (PFA). The standard paraffin embedding and sectioning were performed, followed by hematoxylin and eosin staining. Tissue sections were mounted on slides and sections were analyzed using a compound microscope (Nikon, USA). The slides were also sent to a pathologist in New York Presbyterian Hospital to confirm the observations.

hESC culture, Neuron differentiation and Cell Treatment

Control (WCMC-7) and FXS lines (WCMC-37 and SI-214) were cultured on MEF plated at 12–15,000 cells/cm^2. A hESC medium of DMEM/F12, 20% knockout serum replacement (KSR, Gibco), 0.1 mM 2-mercaptoethanol, 200 mM L-Glutamine, 10 ng/ml FGF-2 (Invitrogen) was changed daily. Cells were passaged using 6 U/ml of dispase in hESC medium, washed and replated at a dilution of 1:5 to 1:10.

Neural induction was performed as described previously (*29*). In brief, stem cells were disaggregated using Accutase (Millipore) for 20 min, washed using hESC medium and pre-plated on 0.1% gelatin for 1 h at 37 °C in the presence of ROCK inhibitor (Y-27632, Tocris Bioscience) to remove MEFs. The nonadherent hESCs were washed and plated on BD Matrigel at a density of 10,000–25,000 cells/cm^2 on Matrigel-coated dishes in MEF-conditioned hESC medium spiked with 10 ng/ml of FGF-2 and ROCK inhibitor. Ideal cell density was found to be 18,000 cells/cm^2. The ROCK inhibitor was withdrawn, and hESCs were allowed to expand in MEF-conditioned hESC medium for 3 days or until they were >90% confluent. The initial differentiation medium conditions included KSR medium with 10 μM TGFβ inhibitor (SB431542, Tocris) and 250 ng/ml of Noggin (R&D). Visible rosettes formed within 5-6 days. Upon 6 days of differentiation, increasing amounts of N2 medium (25%, 50%, 75%) was added to the KSR medium every second day while maintaining 250 ng/ml of Noggin and 10 μM TGF-beta inhibitor. For forebrain neuron differentiations, rosettes were dissociated with accutase at day 12 of differentiation, and plated at low density in neural differentiation medium (DMEM/F12-Glutamax, 1X N2, 1X B27-RA, 20 ng/ml BDNF [Peprotech], 20 ng /ml GDNF [Peprotech], 1mM cAMP [Sigma], 200nM ascorbic acid [Sigma]) onto PORN/laminin-coated plates. Density is critical and the following guidelines were used: 24-well plate, 40,000–60,000 cells per well; 6-well plate, 200,000 cells per well. Half of the medium was gently changed every other day by pipetting.

The CGG-repeat-specific small molecule, 1a, and the control small molecule with no affinity to CGGs, 1f, were described previously (*12*). 1a and 1f were applied to differentiating neurons at a concentration of 10 μM and maintained in culture by freshly adding every other day during the medium change.

Chromatin Immunoprecipitation (ChIP) and Chromatin Isolation by RNA Purification (ChIRP)

ChIP experiments were performed using the EZ-ChIP kit (Millipore, cat # 17-371) following the manufacturer's instructions. For ChIP experiments, 6 million of cells were cross-linked with 1% formaldehyde for 15 min. Upon quenching the unreacted formaldehyde with Glycine and extensive washes with PBS, cells were lysed in SDS buffer supplemented with protease inhibitors (supplied in the kit). Cell lysates were sonicated in Bioruptor (Diagenode) with following settings: high power, 30s pulse, 30s interval, 5 min. This was repeated 9 times to get the range of bands around 500 bp for immunoprecipitation or RNA precipitation. Antibodies used in ChIP were: anti-histone H3 dimethylated on lysine4 (H3K4me2, Millipore) and anti-histone H3 dimethylated on lysine9 (H3K9me2, Millipore). Following the incubation with primary antibodies, antibody/antigen/DNA complex was precipitated by protein G agarose and protein/DNA was eluted on a spin column (Millipore, cat: 17-371). Reverse crosslinking was done at 65ºC for overnight in the presence of 5 M NaCl. Following the removal of RNA and protein by RNAse A and Poteinase K treatments, respectively, the DNA was used in qPCR.

Antisense oligo probes for ChIRP experiments were designed by using the online probe designer at singlemoleculefish.com (Parameters: number of probes = 1 probe /100 bp of RNA length; 2) Target GC% = 45; 3) Oligonucleotide length = 20; 4) Spacing length = 60-80). All probes were biotinylated at the 3' end (Biotin-TEG). 25 probes were generated against the *FMR1* transcript, and all probes were used together in a given ChIRP experiment unless otherwise indicated (100 pmol probe per 1 ml chromatin). Bound *FMR1* promoter was detected by *FMR1* promoter-specific primers that amplify a CpG island located 92-196 bp upstream of the 5'UTR unless otherwise indicated. Sequences of *FMR1* RNA probes are listed in Table S1. In some experiments, different sets of probes that were pooled based on their relative position along the transcript were used for ChIRP (for example, Fig. 4B). ChIRP was performed following a previously described protocol (*30*). In brief, 10 million cells were crosslinked with 1% glutaraldehyde in PBS for 15 min and lysed in 1ml SDS-containing lysis buffer (50 mM Tris-HCl pH 7.0, 10 mM EDTA, 1% SDS, PMSF, protease-inhibitor cocktail II and RNase inhibitor SUPERase-in). Cell lysates were sonicated as described above. 2 ml hybridization buffer (750 mM NaCl, 1% SDS, 50 mM Tris-Cl pH 7.0, 1 mM EDTA, 15% formamide, protease-inhibitor cocktail II and RNAse inhibitor SUPERase-in) was used for 1 ml chromatin. Hybridization buffer contained the probe set of interest at a concentration of 100 pmol probe/1 ml chromatin. Following 4 h of hybridization at 37°C with shaking, samples were added C-1 magnetic beads

(Invitrogen, 100 µL per 100 pmol of probes) and incubated for another 30 min at the same conditions. Beads were separated by magnetic strip, and washed extensively before DNA elution (Wash buffer: 2X NaCl and SSC, 0.5% SDS and PMFS). DNA was eluted by spin column provided in EZ-ChIP kit (Millipore, cat: 17-371) and following manufacturer's instructions. In the experiment to address if *FMR1* RNA and *FMR1* DNA interaction is protein dependent 1 mg/ml trypsin (Invitrogen) was added to the hybridization buffer. In the experiment to address if *FMR1* RNA and *FMR1* DNA make a duplex 5U RNase H (Invitrogen) was added to the chromatin extract (for 15 minutes). To obtain optimized RNase H activity, the chromatin extract was prepared using a previously described non-denaturing buffer (*16*). The sample was then diluted with the hybridization buffer (*30*) containing 1% SDS (final SDS concentration was 0.66%) in order to neutralize RNase H activity. In these experiments sample buffers and hybridization buffers were devoid of protease inhibitors (for trypsin experiment) or RNase inhibitors (for RNase H experiment). Trypsin was inhibited with 2 mg/ml soybean trypsin inhibitor (ATCC) and 1 mM PMSF for 1 h prior to C-1 magnetic beads were applied to the samples.

RNA/cDNA Preparation and Quantitative RT-PCR

Cells were lysed in TRIzol reagent (Invitrogen) and RNA was extracted following the TRIzol protocol using manufacturer's instructions. Purified RNA was incubated with DNAse I (RNase-Free DNase Set, Qiagen) on an RNAeasy mini kit column (Qiagen) to digest genomic DNA. cDNA was transcribed using SuperScript III First-Strand Synthesis SuperMix (Invitrogen) in a 20 µl reaction by using 1 µg of RNA. Real-time quantitative PCR reactions were performed using the iQ SYBR Green Supermix (Bio-Rad) and an Eppendorf Mastercycler ep realplex thermocycler. For each reaction 20 ng cDNA was used. Primers that were used to quantify *FMR1* mRNA and housekeeping gene *GAPDH* mRNA were as follows: *FMR1* F: 5'GTATGGTACCATTTGTTTTTGTG 3', *FMR1* R: 5' CATCATCAGTCACATAGCTTTTTTC 3'; *GAPDH* F: 5' AGCCACATCGCTCAGACACC 3', *GAPDH* R: 5' GTACTCAGCGGCCAGCATCG 3'. Sequences of primers that were used to quantify DNA fragments following ChIP and ChIRP experiments are listed in Table S2.

To access the CGG-repeat length in the *FMR1* 5'UTR in control and premutation lines, we used the Expand Long Template PCR System (Roche Diagnostics), using buffer 2 from the supplied kit and 2 µmol/ml betaine (Sigma-Aldrich). The sequences of primers used in this experiment were as follows: F: 5'GTTTCGGTTTCACTTCCGGT3', R: 5' TCTTCTCTTCAGCCCTGCTA 3'.

The PCR cycling profile to access the repeat length was as follows: denaturation at 98°C for 10 minutes; 10 cycles at 97°C for 35 seconds, 64°C for 35 seconds, 68°C for 4 minutes; 25 cycles at 97°C for 35 seconds, 64°C for 35 seconds, 68°C for 4 minutes, plus a 20-second increment for each cycle; and a final extension at 68°C for 10 minutes.

Knockdown Constructs and Lentivirus Production

Short hairpin sequences were cloned in PRRL lentivirus transfer vector. Sh sequences were as follows: *FMR1* sh1: CAGGTACTTTGTCTAAGAATT, sh2: GTAGTAGACCTTACAGAAATT; *FMR1* scramble control: GGTAATAGATCGTACTCATT; *Dicer* sh: GCAGCTCTGGATCATAATA; *Ago1* sh: GAGAAGAGGTGCTCAAGAA; *Ago2* sh: GTGGGTGTCCTGCGTGAGC; *LacZ* sh: GACTACACAAATCAGCGATT

Lentiviruses were prepared using the third-generation lentiviral system. Four plasmids (transfer vector containing the knockdown sequence and cis-acting sequences for genomic RNA production and packaging, and three plasmids (pLP1, pLP2, and pLP/VSV-G) encoding trans-acting factors [Gag-Pol, Rev, and VSV-G] required for packaging) were co-transfected in HEK 293T cells using CaPO4 precipitation (CalPhos, Clontech). Supernatant containing viral particles was collected and concentrated by ultracentrifugation (22,000 rpm, SW41 Ti rotor, 2 hours, 22°C). The viral pellet was re-suspended in PBS (pH 7.4) containing 1% BSA and stored at -80°C.

Immunohistochemistry and Western Blotting

Neuron cultures were fixed in 4% PFA prior to immunostaining with antibodies specific to human FMRP (mouse anti-human FMRP, Millipore, cat # MAB2160) or β-III tubulin (chicken anti-mouse β-III tubulin, Abcam). FMRP immunostainings were performed by using a peroxidase-based signal amplification system (Tyramid Signal Amplification, TSA, PerkinElmer) according to manufacturer's instructions. TSA enables much higher dilution of primary antibodies than standard protocols. Higher dilution of primary antibodies (1:5000 in our experiments) reduced non-specific interactions and improved the specificity of the staining. When standard immunostaining was carried out, neurons were incubated with primary antibodies diluted in PBS containing 1%Triton X-100 and 10% normal goat serum for overnight at 4°C with gentle agitation. Cells were washed at least 3 x 20 min with PBS following primary antibody incubation. Secondary antibodies were diluted in PBS with 1% Triton X-100 and 10% normal goat serum. Following 2 h of incubation, cells were washed extensively with PBS. Samples

were mounted with aqueous-based mounting solution (Prolong Gold, Invitrogen). Stacks of images were acquired at Zeiss LSM 510 confocal microscopy and processed with LSM 5 image examiner. TUNEL staining was performed using DeadEnd™ Fluorometric TUNEL kit (Promega) following the manufacturer's instructions.

For western blotting, hESCs or neurons were lysed in RIPA buffer (50 mM Tris [pH 8.0], 150 mM NaCl, 1% Nonidet P-40, 0.1% SDS) containing protease (Roche) and phosphatase (Sigma) inhibitor mixtures. Lysates were clarified by centrifugation for 10 min at 4°C. Proteins were resolved by 4% to 12% SDS/PAGE, transferred to nitro- cellulose (Bio-Rad), blocked in 5% (wt/vol) nonfat milk, probed with the appropriate primary and secondary antibodies, and detected by enhanced chemiluminescence (GE Life Sciences).

Determination of T_m

A 2 μM sample of $r(CGG)_{12}$ in 2 mM Na_2HPO_4 (pH 7.0), 45 mM NaCl, and 25 μM Na_2EDTA was heated at 95°C for 1 min and then slowly cooled to room temperature. Compound 1a or 1f was then added to a final concentration of 10 μM (1:1 equivalents of small molecule to 1x1 nucleotide GG internal loops in $r(CGG)_{12}$), and the mixture was incubated at room temperature for 10 min. Optical melting experiments were performed on a Beckman Coulter DU800 UV-Vis spectrophotometer with an attached Peltier heater. A heat rate of 1°C/min was applied, and absorbance at 260 nm was measured. The T_m's were computed as the maximum of the first derivative of the melting (temperature versus absorbance) curves.

Data Analysis

Statistical analysis was performed using Student's t-test and is reported as mean ± SEM. When comparing different treatments on the same cell line, we considered the samples as two samples with equal variance. When comparing different cell lines, we considered the samples as two samples with unequal variance. In all cases, 2-tailed distribution parameter was applied. We considered significant t-test values of *$p < 0.05$, **$p < 0.01$, ***$p < 0.001$, ****$p < 0.0001$.

SUPPLEMENTARY FIGURE LEGENDS

Figure S1. Repeat length of FXS hESC lines and characterization of *FMR1* premutation hESC lines.

The goal of this figure is to characterize two novel *FMR1* premutation hESC lines (WCMC-5 and WCMC-13) that were derived for this study. Our study also utilizes two "full mutation" FXS hESC lines, WCMC-37 and SI-214. We have recently characterized these lines (*8*). "Premutation" *FMR1* alleles contain between ~55 and ~200 CGG repeats. Patients with the premutation allele do not undergo *FMR1* epigenetic silencing—the *FMR1* mRNA and FMRP are still produced. However, mothers with premutation alleles can transmit expanded "full mutation" *FMR1* alleles that have >200 CGG repeats. Each of the WCMC hESC lines were derived from embryos that were tested as part of preimplantation diagnosis for the presence of a possible full mutation *FMR1* allele. Embryos were donated and hESC lines were derived following an approved protocol from the Weill Cornell Embryonic Stem Cell Research Oversight (ESCRO) committee.

To characterize these new hESC lines, we performed experiments to quantify the number of CGG-repeats and to evaluate their stem cell features.

(**A**) Southern blot to determine the length of the CGG repeat tract in the *FMR1* alleles in the FXS hESC lines, WCMC-37 and SI-214. Because of the G/C-rich content, the length of CGG tracts containing greater than 280 CGG repeats cannot be determined by PCR methods (*8*). Therefore, we performed Southern blot using hESCs genomic DNA. Southern blot was performed as described in ref. *8*. In brief, the genomic DNA was digested with *EcoRI* and *EagI*. Double digestion with these endonucleases allows the detection of both active (unmethylated) and inactive (methylated) X-chromosome. *EcoRI* generates a 5.2 kb fragment containing CGG repeats. This fragment is then further digested with *EagI* into 2.6 kb and 2.8 kb fragments (these bands are indistinguishable in our Southern blot) only if *Eag1* site is not methylated. Therefore, a normal female line should produce both a 5.2 kb (derived from unmethylated active X-chromosome) and a 2.8/2.6 kb (derived from methylated X-chromosome) bands following double digestion. Because males only have an active X-chromosome, a normal male should result in only 2.8/2.6 kb band. The control H9 female hESC line represents normal female in this experiment. Both WCMC-37 and SI-214 lines are male as only a single band is observed following *EcoRI* and *EagI* digestion. Both bands are larger than 5.2 kb indicating that these are expanded *FMR1* alleles with more than 450 repeats.

We previously showed that there are a small number of cells in FXS hESC lines that show repeat contraction, resulting in premutation-length alleles (*8*). As discussed in ref. *8*, there are rare, but detectable, repeat contractions and expansions in both FXS lines. Here, we show a representative Southern blot for both FXS hESC lines. A relatively homogeneous repeat length tract is typically seen in these cells consistent with ~450 CGG repeats.

(**B**) CGG-repeat tract length for control hESC line WCMC-7. To determine the number of CGG repeats in the 5'UTR of the *FMR1* allele in the WCMC-7 line, we measured the CGG repeat tract length by an 'expanded long template PCR system' that enables the amplification of G/C rich sequences (see Methods for the details) that are present in a normal range. The PCR primers hybridized 112 bp upstream of the 5' end of the 5'UTR and 1 bp downstream of the 3' end of the CGG repeats in the *FMR1* gene. A normal CGG-repeat tract with approximately 30 repeats would produce a 240 bp band. A control cell line ("Non-FXS lymphoblasts," GM06890 from Coriell Cell Repositories) produced an approximately 240 bp band. As expected, PCR shows that WCMC-7 is a normal line with approximately 30 CGG repeats in the 5'UTR of the *FMR1* gene.

(**C** and **D**) Southern blot to determine the length of the CGG repeat tract in the *FMR1* alleles in the premutation hESC lines, WCMC-5 and WCMC-13. Southern blot was performed as in (**A**). The H9 female hESC line was used as a control. The male WCMC-5 and the female WCMC-13 lines each have one *FMR1* premutation allele with approximately 70 CGG repeats.

To further confirm the number of CGG repeats in these lines, PCR was performed in these lines (see details of Asuragen PCR technique in ref. *8*). AmplideX^{TM} PCR assay and capillary electrophoresis were used to measure the size of the PCR product. Consistent with the Southern blot data, the PCRs from WCMC-5 and WCMC-13 cells show that these cell lines contain 70 and 73 CGG-repeats, respectively. Together, these data indicate that WCMC-7 is a normal line, and WCMC-5 and WCMC-13 are *FMR1* premutation lines.

(**E-G**) WCMC-7, WCMC-5 and WCMC-13 lines display the characteristics of embryonic stem cells.

To determine whether WCMC-7, WCMC-5 and WCMC-13 hESCs have the characteristics of embryonic stem cells, we performed experiments that measure the differentiation capacity of embryonic stem cells. We first tested if these cells can make stem cell-specific colonies and stem cell aggregates (embryoid bodies) in culture. Cells from the three lines were able to

generate colonies and embryoid bodies in culture (**E**). Second, we tested if these cells can form teratomas when injected into mice (see Methods for the details of this experiment) (**F**). Teratomas consist of three germ layers and therefore teratoma formation in mice confirms the pluripotency of a given cell line. Two months following the injection of hESC into mice, we detected teratoma formation by hematoxylin and eosin staining of the teratoma tissue sections. All cell lines were able to generate teratomas that contained different tissue types indicating that cells from WCMC-7, WCMC-5 and WCMC-13 lines are pluripotent. To test if these cells express transcription factors that are exclusive to stem cells and indicate pluripotency, we performed qRT-PCR for *OCT4*, *NANOG* and *REX1* (**G**). All cell lines were positive for these stem cell markers.

Taken together, these data identifies WCMC-7 as a normal hESC line; WCMC-5 and WCMC-13 lines as premutation hESC lines.

Figure S2. Neuronal differentiation leads to marked reduction in *FMR1* mRNA and FMRP expression in WCMC-37 and SI-214 hESCs.

(**A** and **B**) FMRP and *FMR1* mRNA are expressed in WCMC-37 and SI-214 hESCs.

We first sought to determine if FXS lines WCMC-37 (referred as FXS-1 throughout the text) and SI-214 (referred as FXS-2 throughout the text) express FMRP and *FMR1* mRNA when they are undifferentiated. To do this, we performed immunostaining for FMRP (**A**) and qRT-PCR for *FMR1* mRNA (**B**, n=5 per group) in the two FXS hESC lines. FMRP was readily detected by immunofluorescence (green) in control and FXS hESCs. Consistent with this, the expression levels of *FMR1* mRNA were comparable in FXS and control hESCs (**B**). This data indicate that both FMRP and *FMR1* mRNA are expressed in FXS hESCs when they are in an undifferentiated state. Scale bar: 75 μm.

(**C**) Induction of neural differentiation in hESCs.

To study *FMR1* gene silencing in FXS hESCs, we next sought to identify a differentiation protocol that would result in a loss of FMRP expression. *FMR1* gene silencing is dependent on differentiation of hESCs (*7*). To study *FMR1* gene silencing, we used a protocol that converts hESCs into CNS neurons (*29*). In this protocol, differentiating hESCs express the neuroepithelial marker PAX6 at day 6 of neuronal differentiation. While PAX6-positive cells acquire an anterior central nervous system (CNS) identity, PAX6-negative cells turn into neural crest-like cells (*29*). The ratio of PAX6-positive CNS and PAX6-negative neural crest-like cells

can be changed by manipulation of the initial hESC-plating density. High-plating densities result in near-exclusive differentiation toward PAX6-positive cells. In contrast, low densities promote neural crest-like differentiation (*29*). We induced neuronal differentiation in high density cultures. Staining for PAX6 (green) and the pan-neuronal marker PSA-NCAM (red) showed that more than 95% of neural progenitors were positive for the transcription factor PAX6. This data indicate that our neuronal cultures consist of neurons with an anterior CNS identity. Scale bar: 75 μm.

(**D** and **E**) FMRP and *FMR1* expression are downregulated after differentiation of FXS hESCs.

To examine FMRP expression in differentiation-induced *FMR1* gene silencing, we generated neurons from the FXS-1, and FXS-2, as well as control hESC lines. We monitored for FMRP expression by western blot at different time points of neuronal differentiation (**D**). Western blot data showed that in neurons derived from both FXS hESC lines, FMRP was readily detectable up to 36 days, but was clearly reduced at 48 days and not detected at 60 days (**D**). In contrast, FMRP was detected in control neurons at day 60 of differentiation (**D**). Consistent with this data, immunostaining for FMRP showed that FMRP immunofluorescence was not detectable in neurons derived from FXS hESCs at day 60 of differentiation (**E**). This time point for the loss of FMRP in FXS hESCs-derived neurons is consistent with a previous report (*31*). FMRP signal (green) was readily detectable (indicated with arrows) in control neurons at day 60 of differentiation (**E**). β-III tubulin (red) was used as a marker of differentiated neurons. Scale bar: 75 μm.

(**F**) Quantitative RT-PCR for *FMR1* mRNA in control and FXS hESCs during neuronal differentiation.

To address whether the absence of FMRP is due to an alteration in *FMR1* mRNA levels, we quantified *FMR1* mRNA by qRT-PCR in neurons derived from control and FXS hESCs (ES) at different time points of differentiation. Consistent with the FMRP expression, *FMR1* mRNA was readily detected in control neurons. Similar to the loss of protein expression beginning at day 48, qRT-PCR showed that *FMR1* mRNA levels declined in FXS neurons at day 48, and were not detectable at day 60 of differentiation. Data are mean ± SEM, n=4 per condition. When comparing different time points on the same cell line, we considered the samples as two samples with equal variance. 2-tailed distribution parameter was applied, and we established significance as $*p < 0.05$, $**p < 0.01$.

Figure S3. FMRP is expressed in the majority of FXS neurons initially and begins to decline on day 48 with complete loss on day 51.

We sought to determine at which time point between days 45 and 60 of differentiation FXS neurons lose FMRP. In fig. S2D, we showed by western blot that FMRP is highly reduced in FXS neuronal cultures on day 48 and not detected by the end of the 60-day neuronal differentiation protocol (**fig. S2D**). The goal of this figure is to determine exactly when FMRP is completely lost between days 48 and 60. We also asked if all neurons express FMRP and if all FMRP-expressing cells lose FMRP concurrently.

To precisely define when FMRP is completely lost and to determine the cellular distribution of FMRP in our cultures, we stained control and FXS neurons for FMRP (green) and the neuronal marker β-III tubulin (red) on days 45, 48, 51, 54 and 57 of differentiation. Immunostaining allows us to visualize neurons and FMRP expression in individual neurons. In order to analyze as many cells as possible, we cultured neurons at high density for this experiment. As expected, both control and FXS cultures showed similar level of FMRP signal on day 45 of differentiation. All neurons in control and FXS cultures displayed FMRP signal. FMRP staining did not seem to be exclusive to a certain population of neurons. While neurons in control cultures maintained a similar intensity of FMRP signal from day 45 to day 48, FMRP signal was reduced in FXS neurons throughout the culture on day 48 (quantified in **fig. S4**). FMRP signal was not detected in FXS neurons on day 51. These data indicate that FXS hESC-derived neurons lose FMRP by day 51 of differentiation and this occurs in all neurons throughout the culture. Scale bar: 50 μm.

Figure S4. FXS neurons lose FMRP between days 45 and 51 of differentiation.

In the experiment in **fig. S3**, neurons were cultured at high density. Here, we use low density cultures in order to get a better sense of neuronal morphology during the time point of *FMR1* gene silencing. High power images were provided to depict FMRP localization.

(**A**) We performed stainings for FMRP (green) and neuronal marker β-III tubulin (red) in control and FXS neuronal cultures on days 45, 48 and 51 of differentiation.

(**B**) To quantify FMRP and β-III tubulin signals, we performed total fluorescence measurements with Image J. We determined the level of fluorescence in a defined area containing cell bodies. Measurements were obtained in each channel, in order to quantify FMRP and β-III tubulin. To perform the measurements, the integrated density was measured in a given cell-body region.

Then, the mean fluorescence value (background) was measured by selecting a region adjacent to cell bodies. The corrected total fluorescence of FMRP and β-III tubulin in cell bodies was calculated by subtracting the background levels.

Quantifications showed that FMRP levels in 48 day-old FXS neurons dropped more than 50% compared to 45-days-old neurons. On day 51 of differentiation, FMRP levels were reduced >95% compared to day 45 (n=3 biological sets per group, ~100 cell bodies in total 15 regions per condition). Data presented are mean ± SEM. When comparing different time points in the same cell line, we considered the samples as two samples with equal variance. 2-tailed distribution parameter was applied and we established significance as ****$p < 0.0001$. Scale bar: 50 μm for low power images, 30 μm for high power images.

Figure S5. Cell death is not responsible for the loss of FMRP and *FMR1* mRNA in FXS neurons.

In this experiment, we sought to determine if cell death is responsible for FMRP loss in FXS neurons. FMRP is readily detected in FXS neurons until day 48 of differentiation. We showed that FXS neurons lose FMRP between days 48-51 in our differentiation protocol (**fig. S3** and **S4**). However, we cannot exclude the possibility that an increase in cell death between days 45 and 51 contributes to the loss of FMRP signal in FXS cultures. To test this possibility, we measured cell death by TUNEL staining (green) (Promega) in control and FXS cultures during days 45-51 of differentiation.

We observed some dying cells both in control and FXS cultures at these time points of differentiation (indicated by arrows in **A** and quantified in **B**, n=~300 cells per condition). We did not find a significant difference in the rate of cell death between control and FXS neurons at these time points of differentiation. Both cultures contained dying cells at ~15% between days 45 and 51 of neuronal differentiation. This data indicate that cell death is not responsible for the overall FMRP loss seen in FXS neurons by day 51 of neuronal differentiation. Data are mean ± SEM. Scale bar: 100 μm for lower magnification, 25 μm for higher magnification.

Figure S6. Neuronal differentiation represses the *FMR1* promoter in FXS hESC-derived neurons.

We next asked whether the loss of *FMR1* mRNA results from the epigenetic silencing of the *FMR1* gene. We monitored epigenetic modifications of the *FMR1* promoter in control and FXS hESCs before and after neuronal differentiation. To do this, we measured histone H3

dimethylated at lysine 4 (H3K4me2), a mark of transcriptional activation, and histone H3 dimethylated at lysine 9 (H3K9me2), a mark of transcriptional repression, by chromatin immunoprecipitation (ChIP) in control and FXS hESCs before and after neuronal differentiation. *FMR1* promoters in control and FXS hESC have high H3K4me2 (n=4 per condition) and low H3K9me2 levels (n=4 per condition) consistent with the expression of *FMR1* mRNA in these cells. These marks were maintained in neurons derived from control hESCs. However, *FMR1* promoters in FXS hESC-derived neurons contained the repressive mark H3K9me2 and had low levels of H3K4me2. These data indicate that the *FMR1* gene becomes silenced in FXS cells during the 60-day differentiation protocol.

Data are mean ± SEM. When comparing different conditions in the same cell line, we considered the samples as two samples with equal variance. 2-tailed distribution parameter was applied and we established significance as $^{**}p < 0.01$, $^{***}p < 0.001$.

Figure S7. The antisense *FMR1* RNA is not altered by *FMR1* mRNA knockdown, and the CGG-specific compound 1a inhibits unwinding of CGG repeat hairpin structures.

(**A**) Validation of *FMR1* mRNA knockdown by using two short hairpin RNAs against *FMR1* mRNA.

To validate the *FMR1* mRNA knockdown, we measured FMRP levels in control hESCs by western blot on days 3, 4 and 5 following infection with viruses carrying either control shRNA or one of the two *FMR1* mRNA-specific shRNA. To detect FMRP, we used the mouse anti-FMRP antibody from Millipore (cat # MAB2160). Western blot results were visualized as multi-channel fluorescence and single-channel colorimetric images. Florescence multi-channel imaging allows visualizing the protein marker ladder and the protein of interest at the same time. Single channel image has an advantage over multi-channel image in depicting faint bands, including any additional FMRP isoforms. Therefore, we present both images side by side. A band of approximately 75 kDa was readily detected in hESCs which were infected with control shRNA. FMRP was detected in hESCs which were infected with either one of the two *FMR1* mRNA-specific shRNAs up to day 4 following the infection. However, FMRP was lost in hESCs which were infected with *FMR1* mRNA-specific shRNAs on day 5 following the infection. This data indicates that the complete loss of FMRP takes 4-5 days following the application of *FMR1* mRNA-specific shRNAs. This data suggest that FMRP is stable in hESCs for couple of days. Alternatively spliced FMRP isoforms were not readily detectable in these cells.

(**B**) *FMR1* shRNAs do not target antisense *FMR1* RNA.

To determine if shRNAs that knockdown *FMR1* mRNA also target the antisense *FMR1* noncoding RNA (*ASFMR1*), we measured the levels of *ASFMR1* RNA in hESCs upon infection with *FMR1* mRNA-specific shRNAs. *ASFMR1* is transcribed from an alternative promoter at the *FMR1* locus and is about 12,000 nt in length. It partially overlaps with *FMR1* mRNA at the 5'UTR and the first exon (*11*). Although the *FMR1* mRNA-specific shRNAs hybridize outside that region, we wanted to confirm that *ASFMR1* mRNA is not affected by *FMR1* shRNAs. qRT-PCR showed that *ASFMR1* levels were not affected by *FMR1*-specific shRNAs. Data are mean ± SEM (n=3 per condition).

(**C**) Schematic of the hairpin structure formed by CGG repeats.

The predominant structures formed by r(CGG)-repeat RNA under physiological conditions are hairpins with periodically repeating 1x1 nucleotide G-G internal loops (*10*).

(**D**) Small molecule 1a stabilizes $r(CGG)_{12}$ hairpins and prevents their unwinding.

In some of the experiments in this study we used 1a, a small molecule that selectively binds the repeating 1x1 nucleotide G-G internal loop in the $r(CGG)_n$ hairpin to interfere with its function (*12*).

Melting plots of $r(CGG)_{12}$ (black, T_m= 67.2 ± 0.3 °C), $r(CGG)_{12}$ + 5 eq. **1a** (red, T_m= 74.2 ± 0.3 °C, p-value = 0.002) and $r(CGG)_{12}$ + 5 eq. control compound **1f** (blue, T_m= 68.4 ± 0.1 °C, p-value = 0.02) indicated that 1a functions by stabilizing the $r(CGG)_{12}$-hairpin and preventing its thermal denaturation and unwinding.

Figure S8. 1a treatment reverses some of the aberrant transcription in FXS neurons.

FXS is associated with the altered protein synthesis and transcript levels of certain genes in human brain (*32*, *33*). We first sought to determine if these alterations in transcript levels is recapitulated in FXS hESC-derived neurons upon *FMR1* gene silencing. To do this, we harvested FXS neurons on day 60 of differentiation and measured the levels of some of the mRNAs that are known to be either downregulated or upregulated in the brains of FXS patients (*32*) or FXS-hESC derived neurons (*31*). Ref. *32* identified several transcripts, which were differentially expressed in FXS brains compared to controls using microarray analysis and qRT-PCR (*32*). We performed qRT-PCR to measure the levels of the validated transcripts in our FXS as well as control neurons.

Consistent with the data in ref. *32*, we found that the neuronal genes *ASIC2*, *UNC13B*, and *MAP1B* were downregulated, while *GABRD* and *PPP1R9B* were upregulated in FXS neurons upon *FMR1* gene silencing (**A**). We found that the expression levels of *TAU* mRNA are also lower in FXS neurons compared to control neurons consistent with a recent report (*31*). In contrast, the expression levels of the control transcripts *NeuN*, *S100B*, *MAP2* and *SYP* were not significantly different in FXS neurons compared to control neurons on day 60 of differentiation. These data indicate that neurons that are generated from FXS hESCs can recapitulate some aspects of the FXS gene expression phenotype.

We next asked if the small molecule 1a prevents the altered gene expression seen in FXS neurons. We showed in Fig. 1 and Fig. 3 that 1a prevents *FMR1* gene silencing. To determine if 1a prevents the altered levels of the mRNAs mentioned above, we measured the levels of these mRNAs in FXS neurons that were differentiated in the presence of 1a (10 μM) (**B**). The mRNA levels of FXS-associated genes *ASIC2*, *UNC13B*, *TAU*, *MAP1B*, *GABRD* and *PPP1R9B* were comparable between control and FXS hESC-derived neurons upon 1a treatment. The small molecule 1a that prevents *FMR1* gene silencing was able to prevent some of the aspects of the FXS phenotype related to the altered gene expression. 1a treatment did not affect the mRNA levels of the control genes.

These data is consistent with the finding that 1a prevents *FMR1* gene silencing.

Data are mean ± SEM, n=3 per condition. When comparing different conditions in the same cell line, we considered the samples as two samples with equal variance. When comparing different cell lines, we considered the samples as two samples with unequal variance. In all cases, a 2-tailed distribution parameter was applied and we established significance as *$p < 0.05$, **$p < 0.01$.

Figure S9. Targeting the CGG-repeat RNA with a small molecule ligand blocks *FMR1* promoter silencing.

This experiment is similar to Figure 1B, except we show FMRP in FXS neurons by immunofluorescence staining. To determine if the expanded CGG repeats in the *FMR1* mRNA has a role in *FMR1* gene silencing, we used 1a, a small molecule that binds CGG hairpins and prevents their linearization. Differentiating control and FXS hESCs were treated with 1a, or the control compound 1f, throughout the 60 days of differentiation (ES refers to hESC). At the end of the treatment, *FMR1* silencing was evaluated by measuring FMRP by immunofluorescence.

Differentiating FXS hESCs treated with the control compound 1f (10 μM) exhibited *FMR1* promoter silencing, as measured by the loss of FMRP protein. In contrast, FXS hESC-derived neurons that were treated with 10 μM 1a did not lose FMRP expression. These data indicate that the CGG-repeat portion of the *FMR1* mRNA is required for *FMR1* gene silencing. Scale bar: 60 μm.

FMR1 promoter silencing is dependent on terminal differentiation of hESCs. It could be that 1a interferes with neuronal differentiation of FXS hESCs, and thereby leads to inefficient *FMR1* promoter repression. To determine if the small molecule 1a interferes with neuronal differentiation, we stained control and FXS cells for neuronal marker β-III tubulin following the 60 day treatment with 1a. Both control cells and FXS cells that were treated with either 1f or 1a acquired typical neuronal morphology with elaborated neurites and were positive for neuronal marker β-III tubulin. In addition, FXS neurons that were generated in the presence of 1a expressed neuronal-specific transcripts (**fig. S8**).

Together, these data indicate that 1a does not interfere with neuronal differentiation.

Figure S10. The RNAi pathway is not required for *FMR1* gene silencing.

(**A**) Validation of the shRNAs used to knockdown the major components of the RNAi pathway. To validate the efficiency of the knockdown of *Dicer*, *Ago1* and *Ago2* by shRNAs, we measured their mRNA levels following the transduction with corresponding shRNAs. Differentiating hESCs were transduced with lentiviruses expressing shRNAs against *Dicer*, *Ago1* or *Ago2* and mRNA levels were measured by qRT-PCR 4 days following the transduction. *Dicer*, *Ago1* and *Ago2* mRNAs were decreased more than 90% by the corresponding shRNAs indicating that these transcripts can be knocked down with these constructs.

(**B**) The loss of *FMR1* mRNA expression during FXS hESC differentiation occurs normally despite the absence of RNAi pathway components

To determine if the RNAi pathway mediates *FMR1* gene silencing, we first monitored *FMR1* mRNA levels following knockdown of RNAi pathway components in differentiating FXS hESCs. We were concerned that the shRNA could affect the ability of the hESC to differentiate to neurons. At day 12 of neuronal differentiation, cells have already acquired a neuronal identity as confirmed by the prominent expression of neuronal markers such as Pax6 and β-III tubulin. Therefore, we applied lentiviruses expressing shRNAs against *Dicer*, *Ago1* or *Ago2* at day 12 to ensure that the initial steps of the differentiation have already occurred. We measured *FMR1*

mRNA levels at day 60 of differentiation. As expected, FXS neurons that were infected with control shRNA exhibited the expected loss of *FMR1* mRNA at day 60. Cells expressing shRNA constructs that knockdown either *Dicer* or two major RNAi pathway components, *Ago1* and *Ago2,* also exhibited the loss of *FMR1* mRNA at day 60. This data suggest that the RNAi pathway is not required for *FMR1* gene silencing.

(**C**) Epigenetic silencing of the *FMR1* gene during FXS hESC differentiation occurs normally despite the absence of RNAi pathway components.

To determine if the RNAi pathway has a role in *FMR1* gene silencing, we measured histone marks on the *FMR1* promoter following knockdown of RNAi pathway components. As expected, *FMR1* promoters in FXS were silenced, as determined by the low levels of H3K4me2 and high levels of H3k9me2 in cells expressing control shRNA. Knockdown of either *Dicer* or two major RNAi pathway components, *Ago1* and *Ago2*, did not prevent *FMR1* promoter silencing in neurons derived from FXS hESCs. These cells acquired heterochromatin histone marks similar to FXS neurons transduced with control shRNA.

Together, these data indicate that *FMR1* promoter silencing does not occur through a Dicer-directed pathway.

Figure S11. *FMR1* mRNA interacts with the *FMR1* promoter only at day 45 of the neuronal differentiation protocol but not at other time points.

To determine if *FMR1* mRNA interacts with the *FMR1* promoter, we performed chromatin isolation by RNA purification (ChIRP) at different time points throughout the differentiation. Recently, various noncoding RNAs have been shown to mediate transcriptional silencing by interacting with gene promoters. To test if such an interaction also occurs between *FMR1* mRNA and the *FMR1* promoter at any time during differentiation, we performed ChIRP at days 12, 24, 36, 45, 60 and measured the amount of *FMR1* DNA that was pulled down by biotinylated oligoprobes against *FMR1* mRNA. ChIRP revealed that *FMR1* mRNA interacts with the *FMR1* promoter, and this interaction occurs at around day 45 of differentiation in FXS neurons. Binding was not seen at earlier time points (day 12, 24, or 36) or afterwards (day 60). The absence of *FMR1* mRNA binding to the *FMR1* promoter at day 60 is consistent with the absence of *FMR1* mRNA at this time point. As a control, we monitored the binding of *FMR1* mRNA to the *GAPDH* and *β-III tubulin* promoter. Markedly reduced *FMR1* mRNA was detected at these promoters by ChIRP. In control hESC-derived neurons, there was minimal association

of the *FMR1* transcript with the *FMR1* promoter at any time point during the differentiation protocol.

This data indicates that *FMR1* mRNA transiently associates with the promoter region of the *FMR1* gene.

Data are mean ± SEM, n=3 per condition. When comparing different conditions in the same cell line, we considered the samples as two samples with equal variance. When comparing different cell lines, we considered the samples as two samples with unequal variance. In all cases, a 2-tailed distribution parameter was applied and we established significance as **p < 0.01, ***p < 0.001.

Figure S12. The CGG-repeat tract is not required for *FMR1* gene silencing during the first 30 days of neuronal differentiation.

To test if *FMR1* mRNA binding to the *FMR1* gene is necessary for *FMR1* promoter silencing, we interfered with the unfolding of CGG repeats in the *FMR1* mRNA with 1a. 1a prevents *FMR1* mRNA binding to the *FMR1* promoter (**Fig. 2C**). To precisely define the temporal sensitivity of promoter silencing to 1a, we applied 1a to differentiating hESCs at different time points of differentiation. In this experiment, we selectively applied 1a to differentiating cells during days 1-30 of the differentiation protocol (see **Fig. 3** for the other time point).

(**A**) Schematic representation of 1a treatment in differentiating hESCs. The CGG-specific compound 1a (10 µM) or control compound 1f (10 µM) were applied to differentiating control and FXS hESCs during the first 30 days of neuronal differentiation. The drugs were withdrawn at day 31 and cultures were maintained for another 30 days. The samples were collected at day 60 of differentiation for FMRP western blotting, *FMR1* qRT-PCR and ChIP experiments.

(**B-D**) 1a treatment during the first half of neuronal differentiation does not prevent *FMR1* gene silencing.

To evaluate *FMR1* gene silencing upon 1a treatment, we monitored FMRP (**B**), measured *FMR1* mRNA levels (**C**, n=3 per condition) and histone modifications (**D**, n=3 per condition).

Application of 1a (10 µM) during days 1-30 of differentiation did not prevent *FMR1* promoter silencing. Data are mean ± SEM.

Figure S13. The *FMR1* mRNA requirement for *FMR1* gene silencing coincides with the time *FMR1* mRNA interacts with the *FMR1* promoter.

To determine if the binding of *FMR1* mRNA to the *FMR1* gene leads to *FMR1* gene silencing, we tested if the temporal requirement for *FMR1* mRNA in *FMR1* promoter silencing coincides with the binding of *FMR1* mRNA to the *FMR1* gene. The *FMR1* mRNA is required for *FMR1* gene silencing (see **Fig. 1A**) as the knockdown of *FMR1* by shRNA throughout the 60 days of differentiation interferes with silencing. The onset of *FMR1* gene silencing, which occurs at ~day 48 (see **fig. S2D-F**) coincides with the time when the *FMR1* mRNA is first seen to bind the *FMR1* gene. This is consistent with the idea that *FMR1* mRNA binding to the gene causes silencing.

To more precisely define the temporal requirement for *FMR1* mRNA in *FMR1* promoter silencing, we applied *FMR1*-specific shRNAs to FXS hESCs beginning at day 31 of differentiation and monitored the histone marks on the *FMR1* promoter at day 60. Knockdown of the *FMR1* mRNA between 31-60 days also prevented silencing in FXS neurons, as *FMR1* promoters in these cells were associated with euchromatic histone marks.

This suggests that *FMR1* mRNA is not required for gene silencing in the first 30 days, but that the gene silencing process occurs in the second 30-day period. This is the same time when it binds to the *FMR1* gene. This data together with the data in **Fig. 3** and **fig. S12,** further supports the idea that *FMR1* mRNA binding to the *FMR1* gene causes silencing.

Data are mean ± SEM, n=3 per condition. When comparing different conditions in the same cell line, we considered the samples as two samples with equal variance. 2-tailed distribution parameter was applied, and we established significance as ***p < 0.001, ****p < 0.0001.

Figure S14. *FMR1* mRNA binds to the *FMR1* promoter and initiates *FMR1* gene silencing following withdrawal of 1a from FXS neurons at day 60 of differentiation.

We sought to determine if *FMR1* promoter repression could still take place when FXS neurons pass the critical time point at which *FMR1* gene silencing occurs. We showed that *FMR1* gene silencing occurs between days 48-51 of neuronal differentiation protocol. When differentiating FXS hESCs are treated with 1a during days 31-60 of differentiation, we see that *FMR1* gene silencing is prevented in these 60 days old cells (**Fig. 3**). But those experiments did not address if *FMR1* gene silencing could occur following the withdrawal of 1a after day 60.

To test if *FMR1* gene silencing can occur following withdrawal of 1a, we first treated FXS cells with 1a during days 31-60, and then removed 1a from cultures during days 61-70 of differentiation. Cells were harvested at day 70 (See schematic for the experimental paradigm in **A**). As a control, we treated control and FXS cells with 1f or 1a up to day 70 of differentiation. All cells used in this experiment were harvested at day 70 of neuronal differentiation. We evaluated *FMR1* gene silencing by monitoring FMRP (**A**) and measuring *FMR1* mRNA levels (**B**). As expected, FXS neurons that were treated with 1a up to day 70 maintained FMRP (**A**) and *FMR1* mRNA (**B**) expression consistent with our finding that 1a prevents *FMR1* promoter repression. In contrast, treatment with 1a up to day 60 followed by withdrawal of 1a during days 61-70 resulted in *FMR1* gene silencing as this treatment resulted in loss of FMRP (**A**) and *FMR1* mRNA (**B**, n=3 per condition).

These data indicate that 1a is continuously required to maintain *FMR1* in the silenced state, and silencing can occur after days 48-51 of the differentiation period. Data are mean ± SEM. Scale bar: 75 μm.

Figure S15. 1a cannot reverse *FMR1* promoter repression in FXS lymphocytes.

In this experiment we sought to determine if 1a is capable to derepress *FMR1* promoter in FXS cells. In figure 1 and 3, we showed that 1a treatment prevents the *FMR1* gene silencing in differentiating FXS hESCs by interfering with the binding of *FMR1* mRNA with the *FMR1* gene. An intriguing question is: Can 1a reverse *FMR1* promoter repression in FXS cells that already switched off *FMR1* gene?

To test if 1a can reverse *FMR1* promoter repression, we treated FXS lymphocytes (GM06852 from Coriell Cell Repositories) with 1a for 7 days and monitored *FMR1* gene silencing. We evaluated *FMR1* gene silencing by monitoring FMRP (**A**), *FMR1* mRNA (**B**) and histone marks (**C**) following treatment with either the control molecule 1f or the CGG-specific molecule 1a. In these experiments we also used non-FXS lymphocytes (GM06890 from Coriell Cell Repositories) as a control. As expected, FXS cells that were treated with 1f did not contain FMRP and *FMR1* mRNA. Consistent with this, *FMR1* promoters in FXS lymphocytes were associated with low levels of H3K4me2 and high levels of H3K9me2 following 1f treatment (**C**). 1a treatment did not result in appearance of either FMRP (**A**) or *FMR1* mRNA (**B**) in FXS lymphocytes. Similarly 1a did not cause the *FMR1* promoter to switch to active epigenetic marks. FXS cells maintained low levels of H3K4me2 and high levels of H3K9me2 despite 1a treatment (**C**).

These experiments indicate that 1a cannot activate the *FMR1* promoter once epigenetic silencing has taken place.

Data are mean ± SEM, n=3 per condition. When comparing different treatments in the same cell line, we considered the samples as two samples with equal variance. When comparing different cell lines, we considered the samples as two samples with unequal variance. In all cases, a 2-tailed distribution parameter was applied and we established significance as *p < 0.05, **p < 0.01, ***p < 0.001.

Figure S16. Model to explain the basis for the ChIRP signal on either side of the CGG repeats.

To determine where the *FMR1* mRNA binds to the *FMR1* gene, we measured the ChIRP signal along a 1200 bp region both upstream and downstream of the genomic CGG repeat (**Fig. 4C**). Because of the exclusive G/C content in the CGG repeat (~1300 bp), it is not possible to amplify this region. The ChIRP signal was primarily detected on either side of the genomic CGG repeat, and with markedly reduced signals at sites away from the repeat region (**Fig. 4C**).

The ChIRP results are interesting for two reasons: first, why is the ChIRP signal detected on either side of the CGG-repeat portion in the *FMR1* gene? This may reflect binding of the *FMR1* transcript to the genomic CGG repeat. This region comprises ~1300 bp in the *FMR1* gene in both FXS hESC lines. Because sheared DNA is ~500 bp in the ChIRP protocol, DNA fragments can come from either upstream or downstream of the CGG repeat and still contain a portion of the CGG repeat. Thus, primers directed to these CGG repeat-adjacent regions can produce a ChIRP signal if the CGG repeat sequence itself is the binding site of the *FMR1* mRNA. Thus, binding of the *FMR1* transcript to the genomic CGG-repeat sequence could explain the promoter-scanning ChIRP results. The second interesting feature of the ChIRP experiment is that *FMR1* mRNA exhibits a ChIRP signal over a broad expanse of DNA, comprising at least 1300 bp, since the genomic CGG repeat in both the FXS hESC lines is this length. In principle, if the *FMR1* mRNA was binding to one specific site in the genome, then the ChIRP signal should have been localized to one discrete area. This scheme proposes an explanation for this phenomenon, based on the idea that the mRNA is likely to be hybridized to the DNA in a specific orientation, which will result in the asymmetric ChIRP.

Each of the three panels shows the *FMR1* mRNA hybridized to the complementary DNA strand of the CGG repeat. The repeat portions of both the mRNA and DNA are shown in green. The

different panels show the *FMR1* mRNA hybridized in different positions along the genomic repeats. In panel 1, the *FMR1* mRNA repeat is hybridized along its length with the DNA. In panel 2, just a small portion is hybridized to the 3' end of the genomic repeat. In panel 3, a small portion of the *FMR1* mRNA repeat is bound to the 5' end of the repeat. In each case, the part of the mRNA that is pulled down using biotinylated complementary oligonucleotides is closer to the 3' side of the genomic repeat tract than the 5' side of the genomic repeat tract.

FMR1 mRNA and *FMR1* gene interaction at the CGG-repeat tract is unlikely to be due to the formation of an RNA-DNA•DNA triplex, which typically comprise U-A•T base triples. These residues are not found in the repeat sequences. Additionally, the C-G•G base triple is not stable at physiologic pH (*34*). Thus, highly stable RNA-DNA triplexes are not expected to form from these sequences.

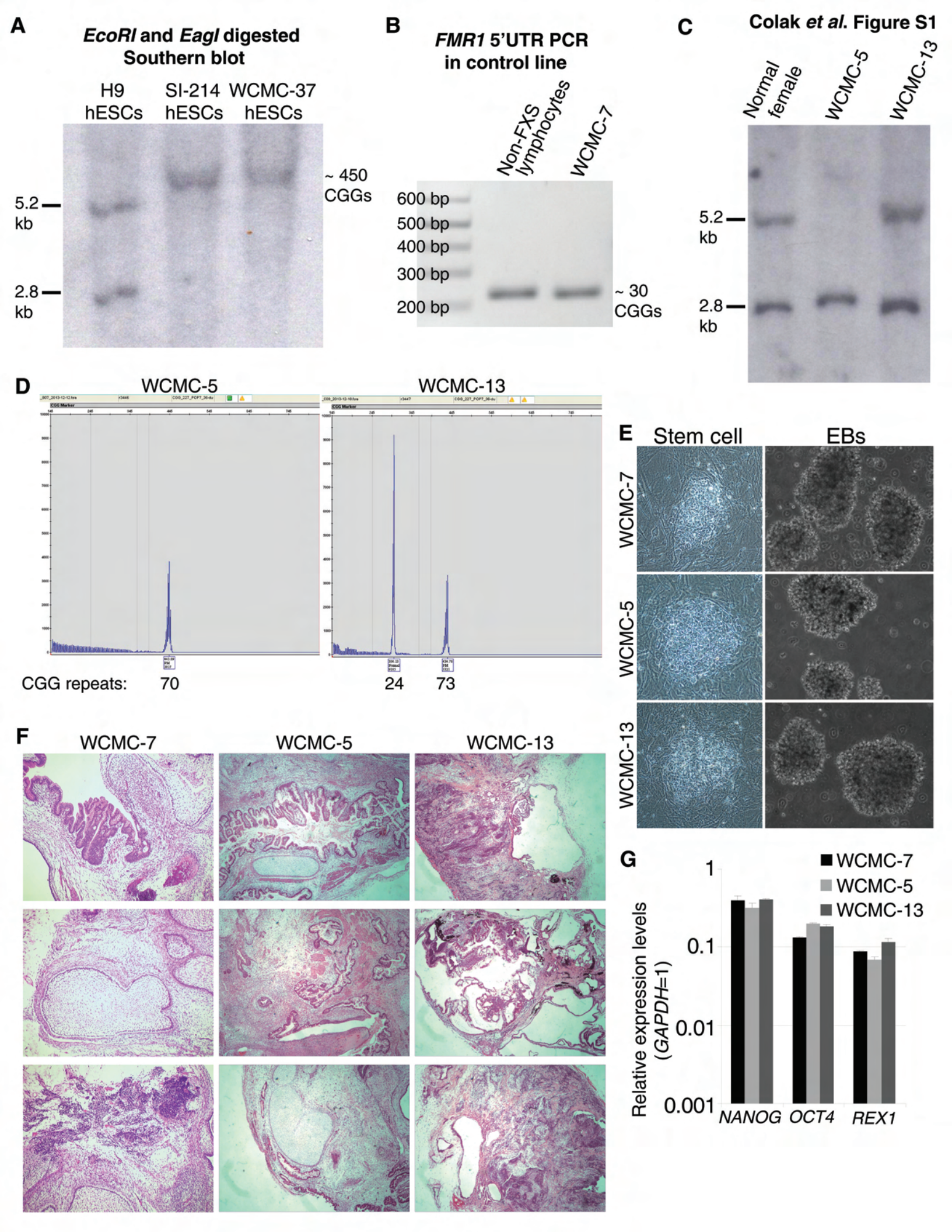
A
EcoRI and EagI digested Southern blot
H9 hESCs
SI-214 hESCs
WCMC-37 hESCs
5.2 kb
2.8 kb
~ 450 CGGs
B
FMR1 5'UTR PCR in control line
Non-FXS lymphocytes
WCMC-7
600 bp
500 bp
400 bp
300 bp
200 bp
~ 30 CGGs
C
Colak et al. Figure S1
Normal female
WCMC-5
WCMC-13
5.2 kb
2.8 kb
D
WCMC-5
WCMC-13
CGG repeats: 70 24 73
E
Stem cell
EBs
WCMC-7
WCMC-5
WCMC-13
F
WCMC-7
WCMC-5
WCMC-13
G
WCMC-7
WCMC-5
WCMC-13
Relative expression levels (GAPDH=1)
1
0.1
0.01
0.001
NANOG
OCT4
REX1

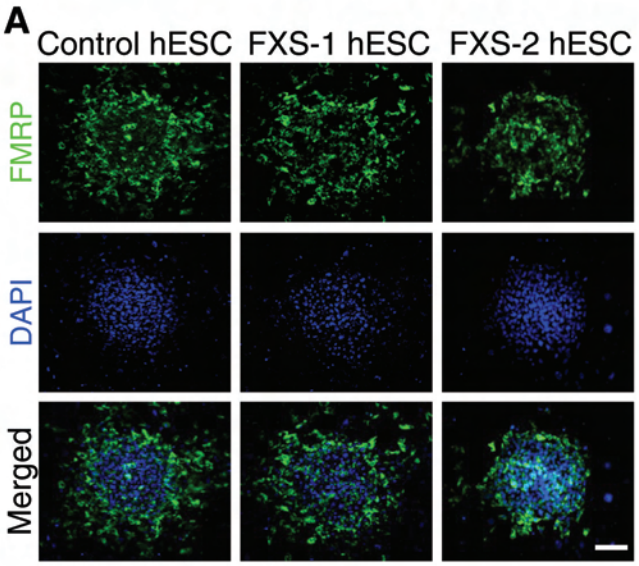
A
Control hESC
FXS-1 hESC
FXS-2 hESC
FMRP
DAPI
Merged

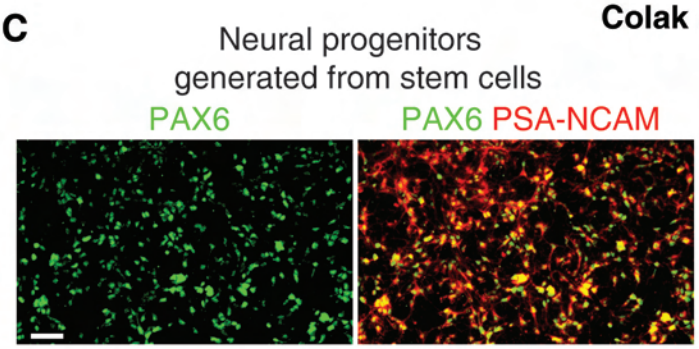
C
Neural progenitors generated from stem cells
PAX6
PAX6 PSA-NCAM

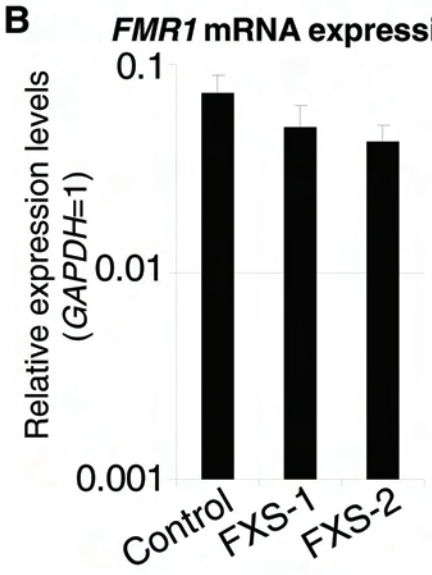
B
FMR1 mRNA expression
Relative expression levels (GAPDH=1)
0.1
0.01
0.001
Control
FXS-1
FXS-2

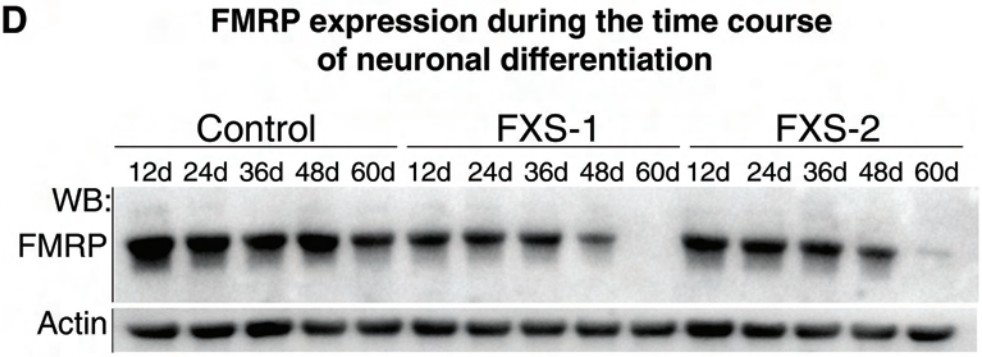
D
FMRP expression during the time course of neuronal differentiation
Control
FXS-1
FXS-2
12d 24d 36d 48d 60d 12d 24d 36d 48d 60d 12d 24d 36d 48d 60d
WB:
FMRP
Actin

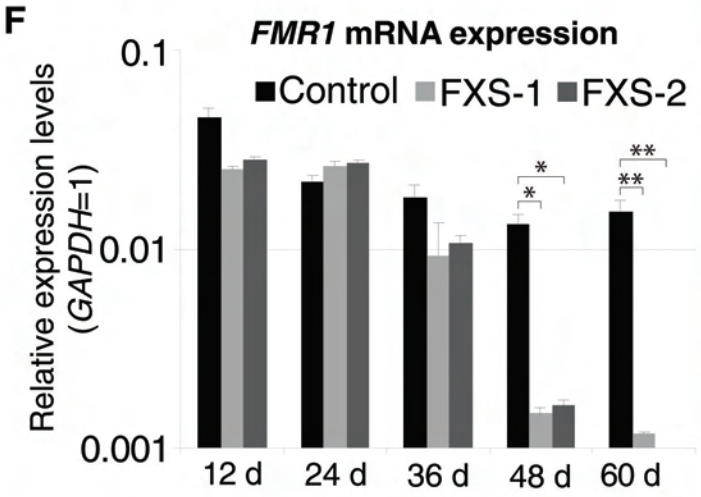
F
FMR1 mRNA expression
Control
FXS-1
FXS-2
Relative expression levels (GAPDH=1)
0.1
0.01
0.001
*
*
**
**
12 d
24 d
36 d
48 d
60 d

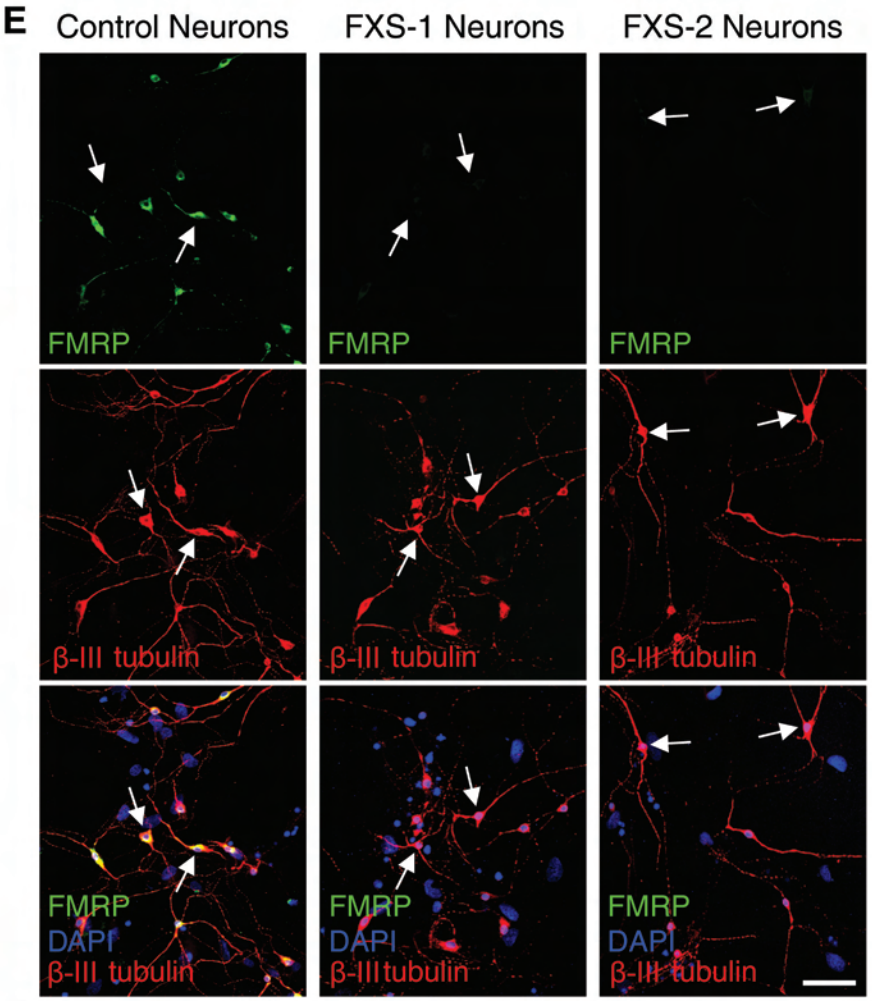
E
Control Neurons
FXS-1 Neurons
FXS-2 Neurons
FMRP
β-III tubulin
DAPI

Colak *et al.* Figure S3

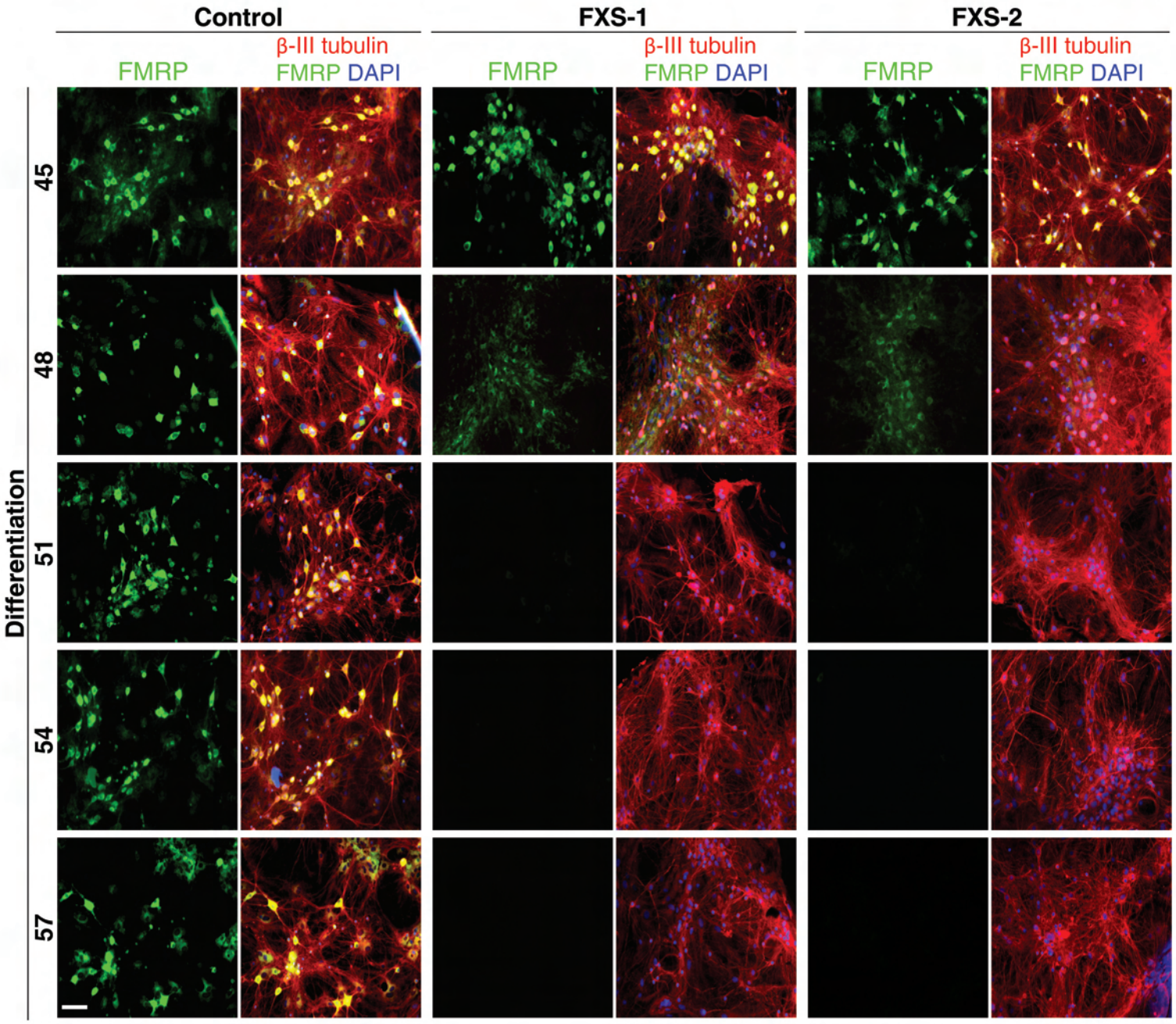

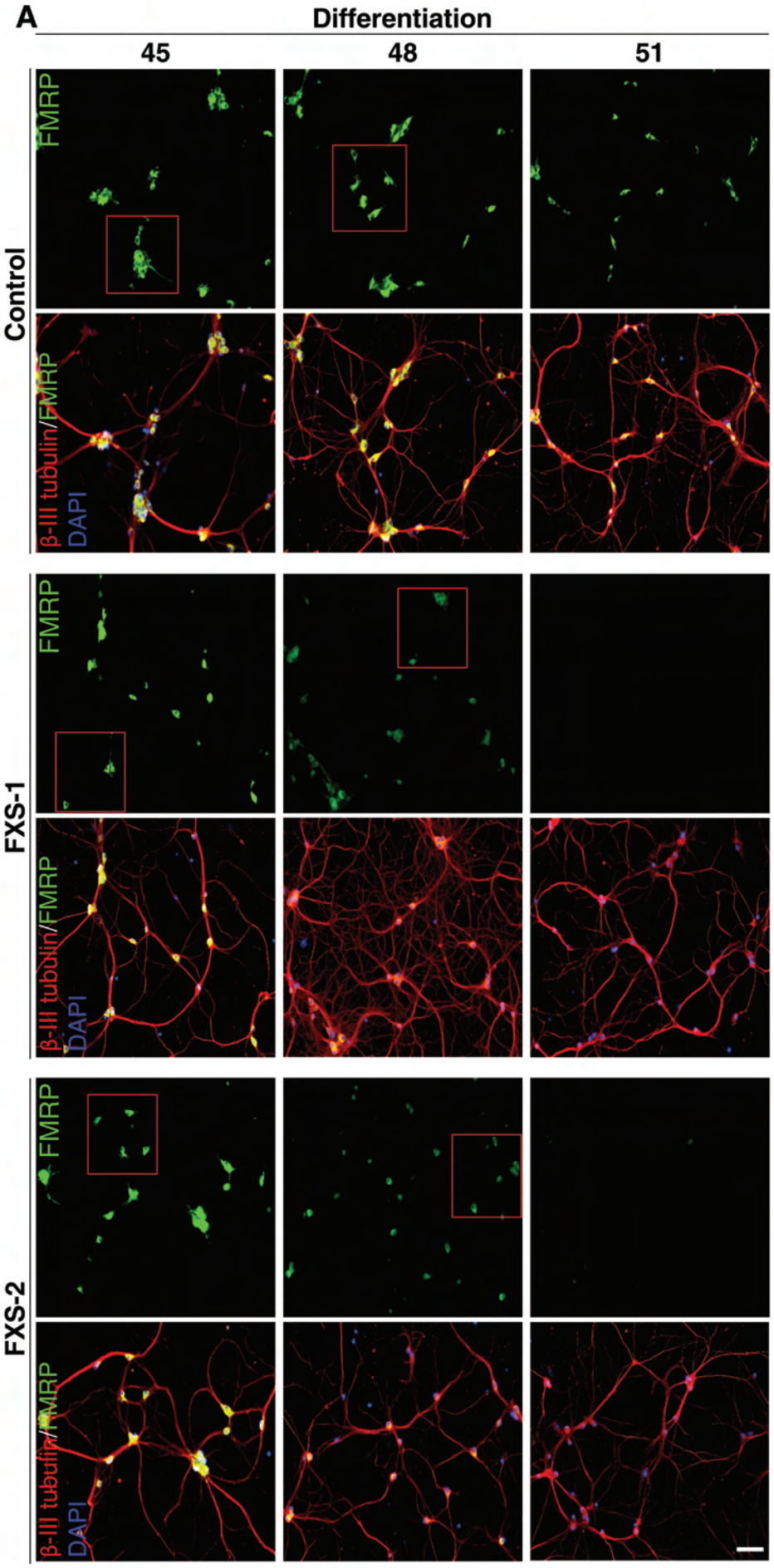
A
Differentiation
45
48
51
Control
FXS-1
FXS-2
FMRP
β-III tubulin/FMRP
DAPI

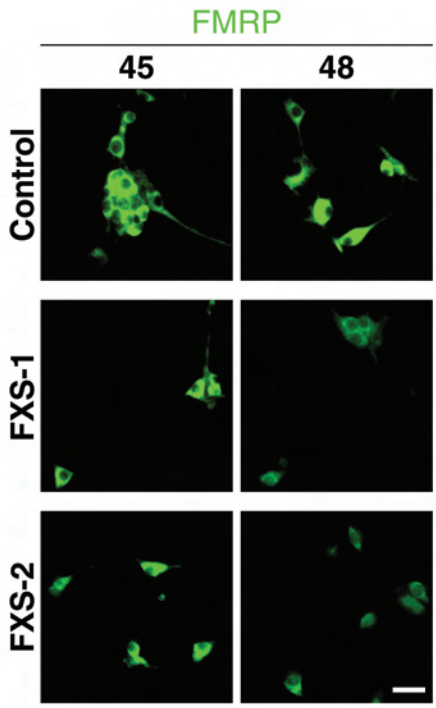
FMRP
45
48
Control
FXS-1
FXS-2

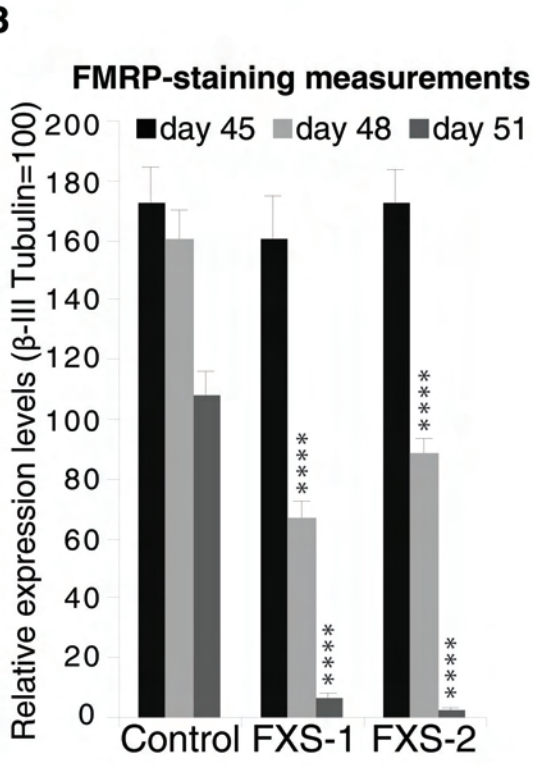
B
FMRP-staining measurements
day 45
day 48
day 51
Relative expression levels (β-III Tubulin=100)
200
180
160
140
120
100
80
60
40
20
0
****
Control
FXS-1
FXS-2

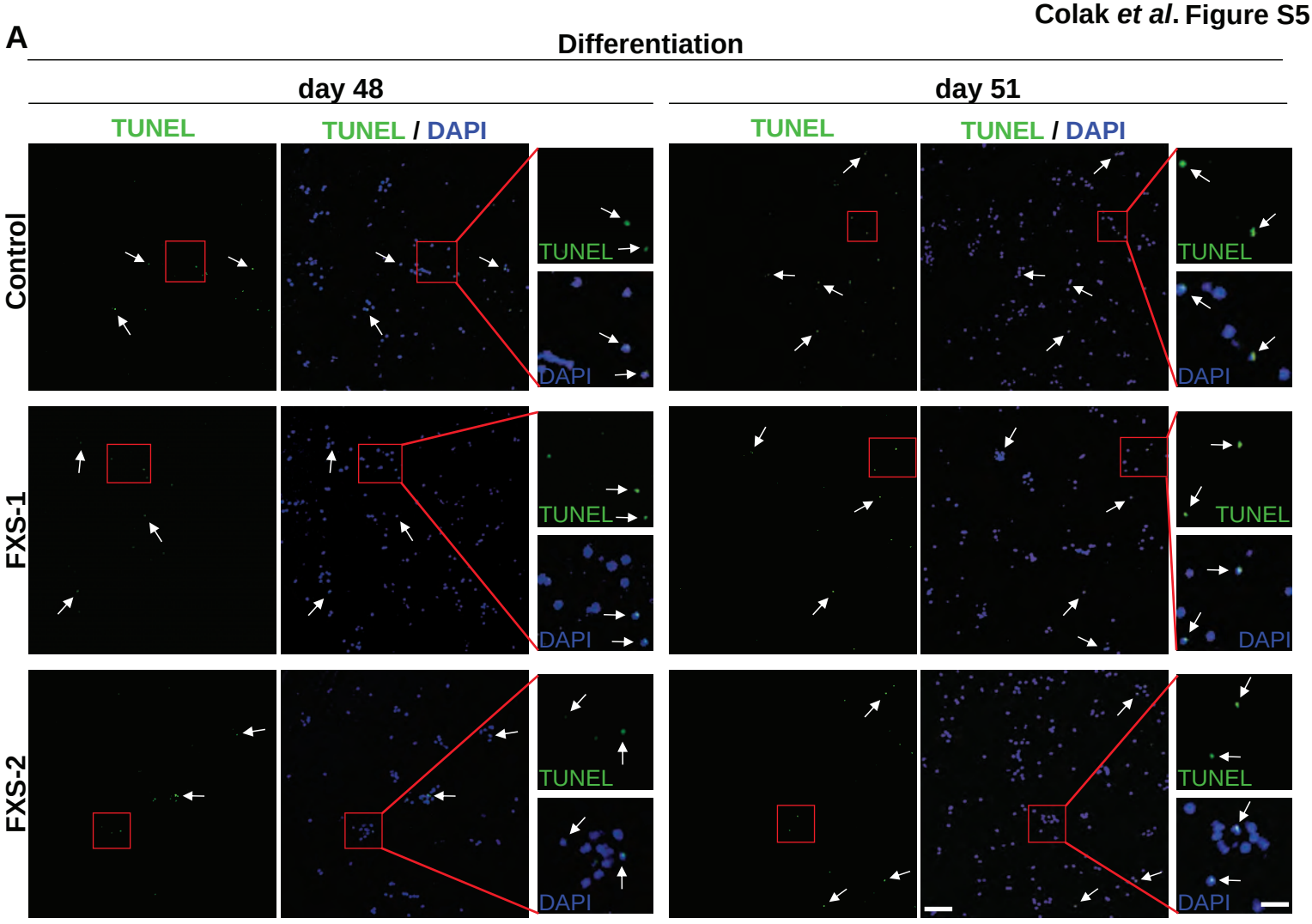
A
Differentiation
day 48
day 51
TUNEL
TUNEL / DAPI
TUNEL
TUNEL / DAPI
Control
FXS-1
FXS-2
TUNEL
DAPI

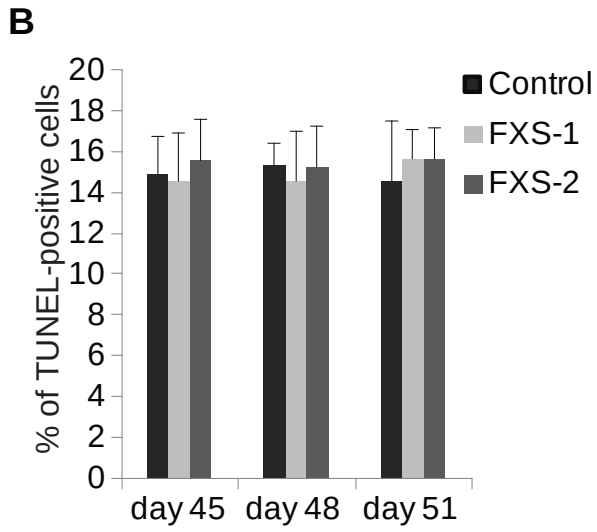
B
% of TUNEL-positive cells
20
18
16
14
12
10
8
6
4
2
0
day 45
day 48
day 51
Control
FXS-1
FXS-2

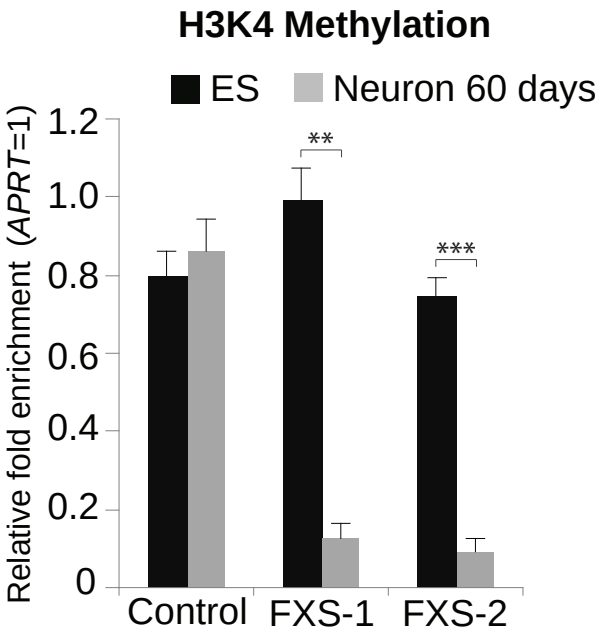
H3K4 Methylation
ES
Neuron 60 days
Relative fold enrichment (APRT=1)
1.2
1.0
0.8
0.6
0.4
0.2
0
**
***
Control
FXS-1
FXS-2

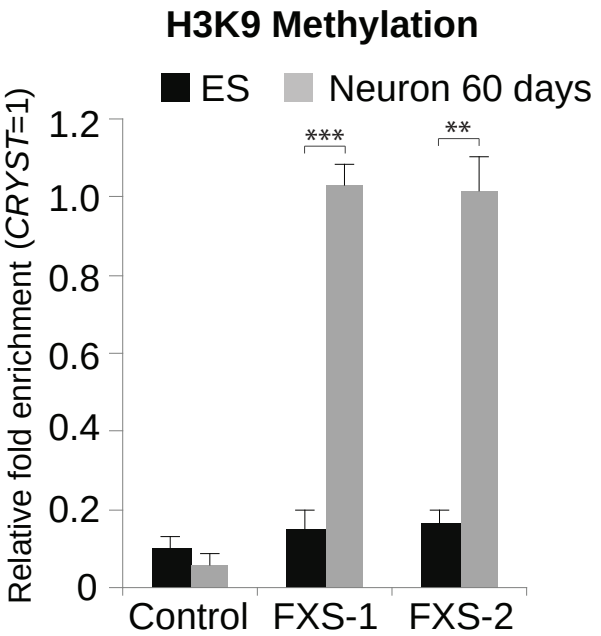
H3K9 Methylation
ES
Neuron 60 days
Relative fold enrichment (CRYST=1)
1.2
1.0
0.8
0.6
0.4
0.2
0
***
**
Control
FXS-1
FXS-2

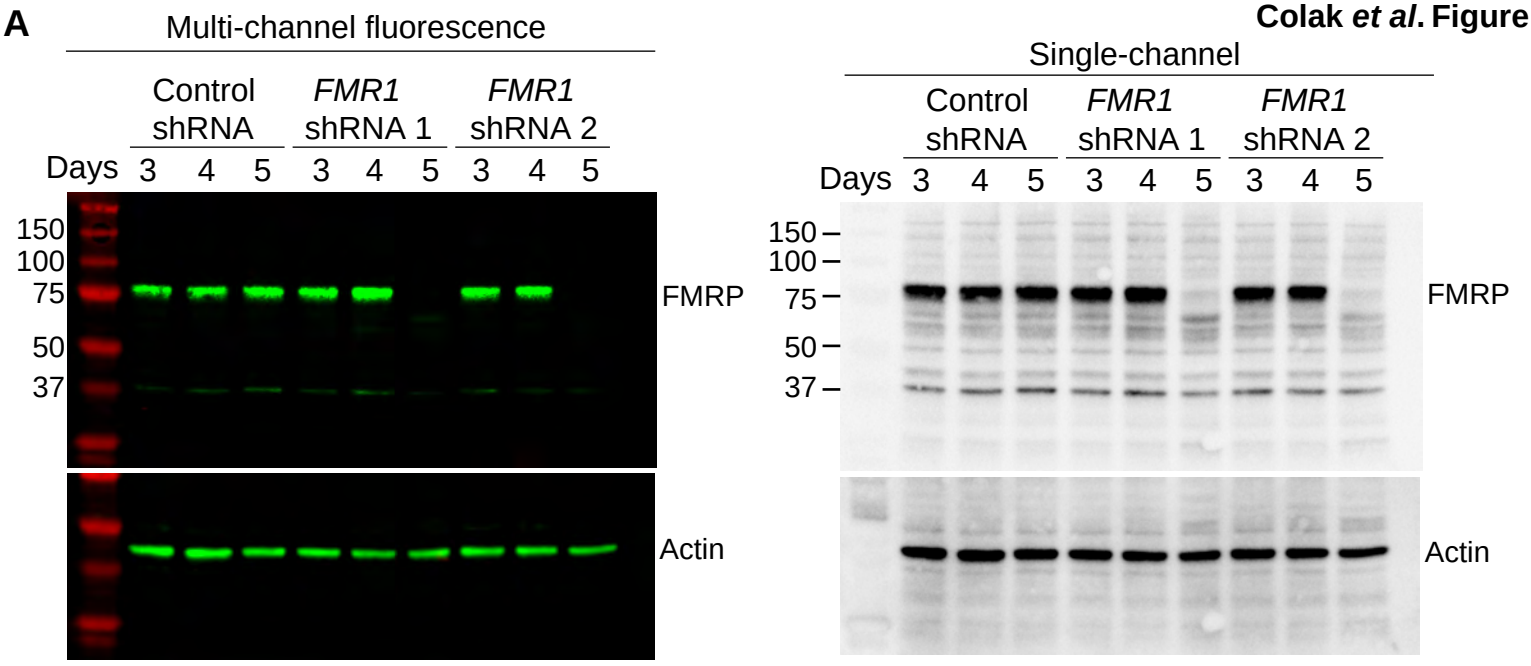
A
Multi-channel fluorescence
Control shRNA
FMR1 shRNA 1
FMR1 shRNA 2
Days 3 4 5 3 4 5 3 4 5
150
100
75
50
37
FMRP
Actin
Single-channel
Control shRNA
FMR1 shRNA 1
FMR1 shRNA 2
Days 3 4 5 3 4 5 3 4 5
150
100
75
50
37
FMRP
Actin

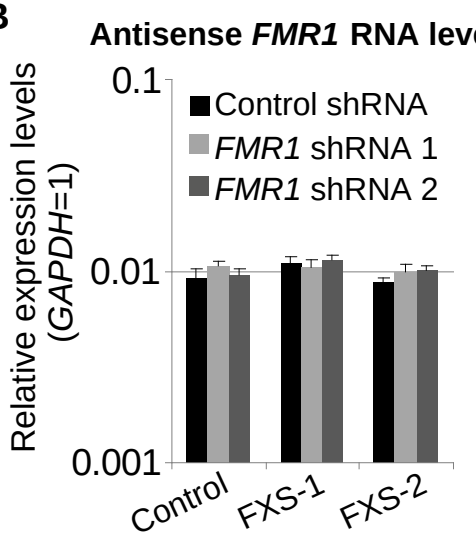
B
Antisense FMR1 RNA levels
Relative expression levels (GAPDH=1)
0.1
0.01
0.001
Control shRNA
FMR1 shRNA 1
FMR1 shRNA 2
Control
FXS-1
FXS-2

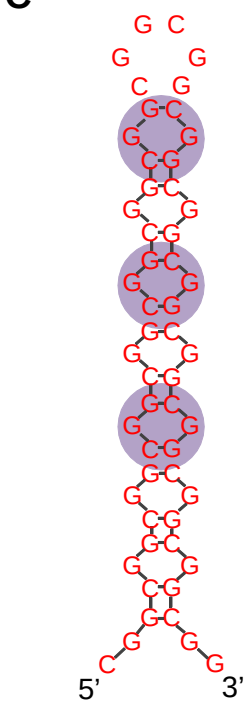
C
G C
G G
C G
G-C
G G
C-G
G-C
G G
C-G
G-C
G G
C-G
G-C
G G
C-G
G-C
G G
C-G
G-C
G G
C-G
G-C
C G G
5'
3'

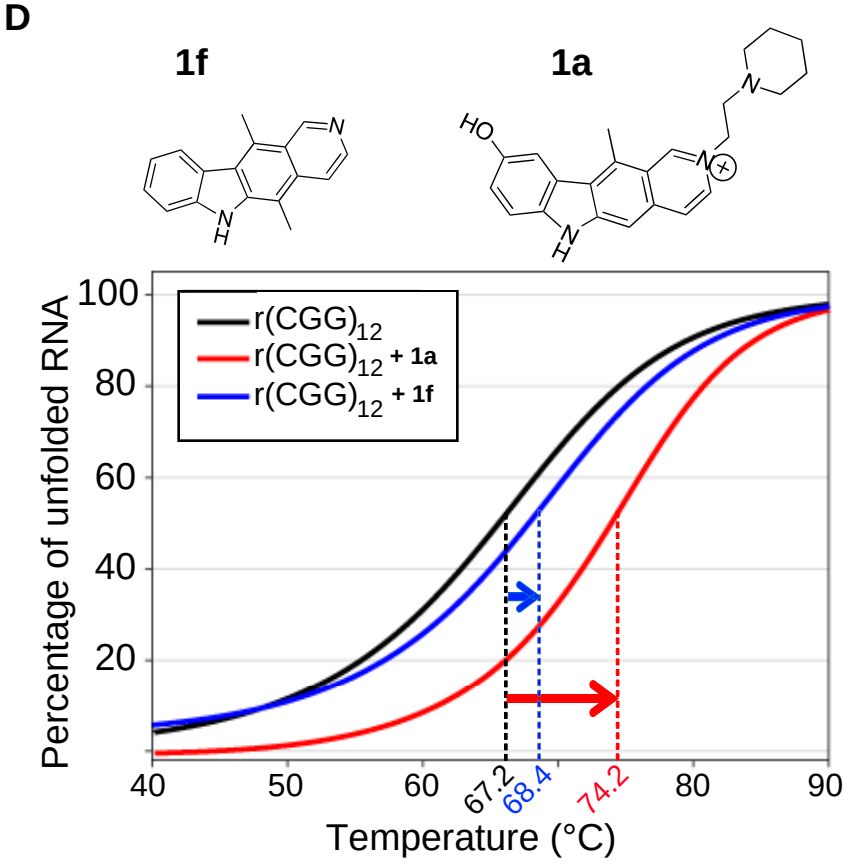
D
1f
1a
HO
N
H
N
N
+
Percentage of unfolded RNA
100
80
60
40
20
r(CGG)12
r(CGG)12 + 1a
r(CGG)12 + 1f
40
50
60
67.2
68.4
74.2
80
90
Temperature (°C)

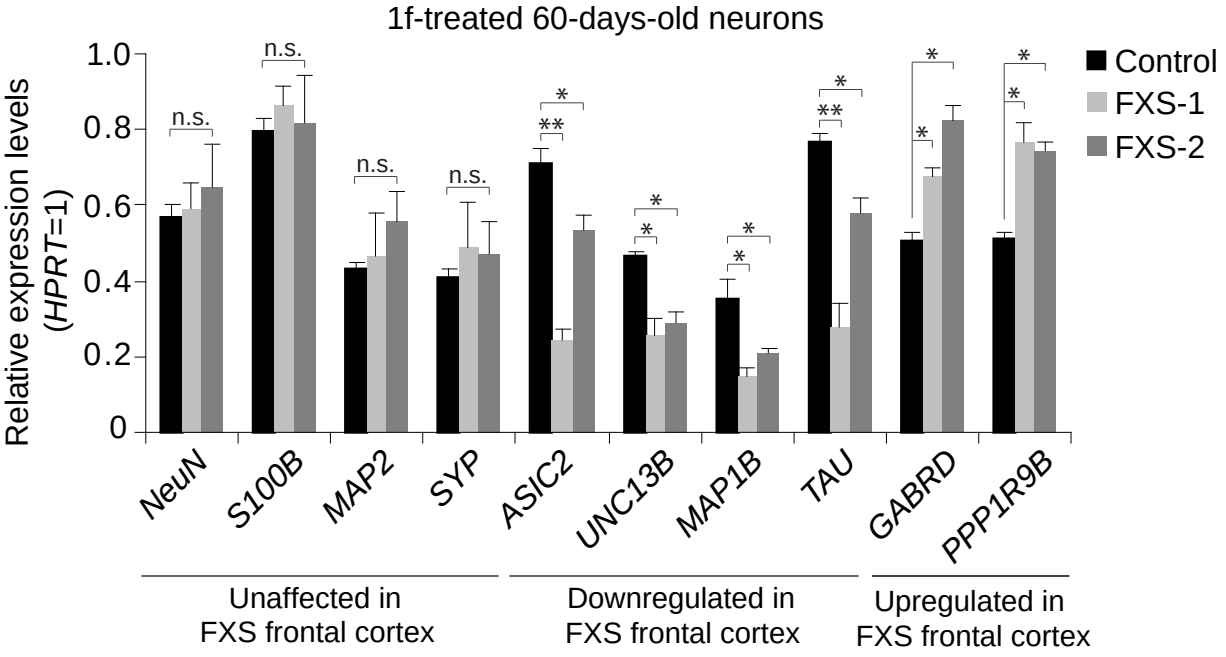
1f-treated 60-days-old neurons
Relative expression levels (HPRT=1)
1.0
0.8
0.6
0.4
0.2
0
Control
FXS-1
FXS-2
n.s.
*
**
NeuN
S100B
MAP2
SYP
ASIC2
UNC13B
MAP1B
TAU
GABRD
PPP1R9B
Unaffected in FXS frontal cortex
Downregulated in FXS frontal cortex
Upregulated in FXS frontal cortex

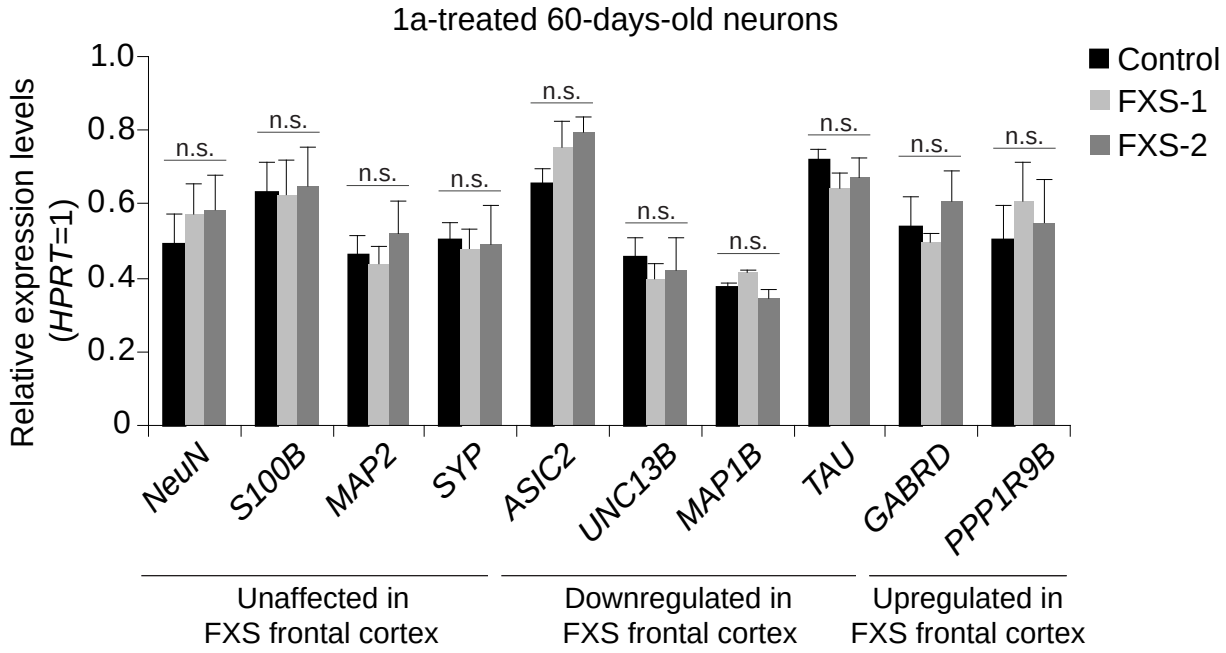
1a-treated 60-days-old neurons
Relative expression levels (HPRT=1)
1.0
0.8
0.6
0.4
0.2
0
Control
FXS-1
FXS-2
n.s.
NeuN
S100B
MAP2
SYP
ASIC2
UNC13B
MAP1B
TAU
GABRD
PPP1R9B
Unaffected in FXS frontal cortex
Downregulated in FXS frontal cortex
Upregulated in FXS frontal cortex

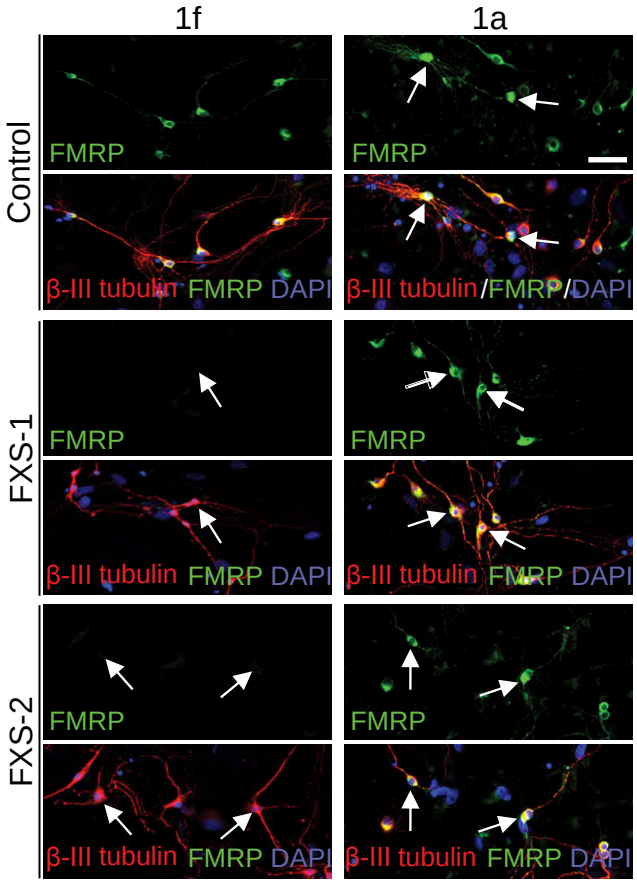
1f
1a
Control
FXS-1
FXS-2
FMRP
β-III tubulin FMRP DAPI
β-III tubulin/FMRP/DAPI

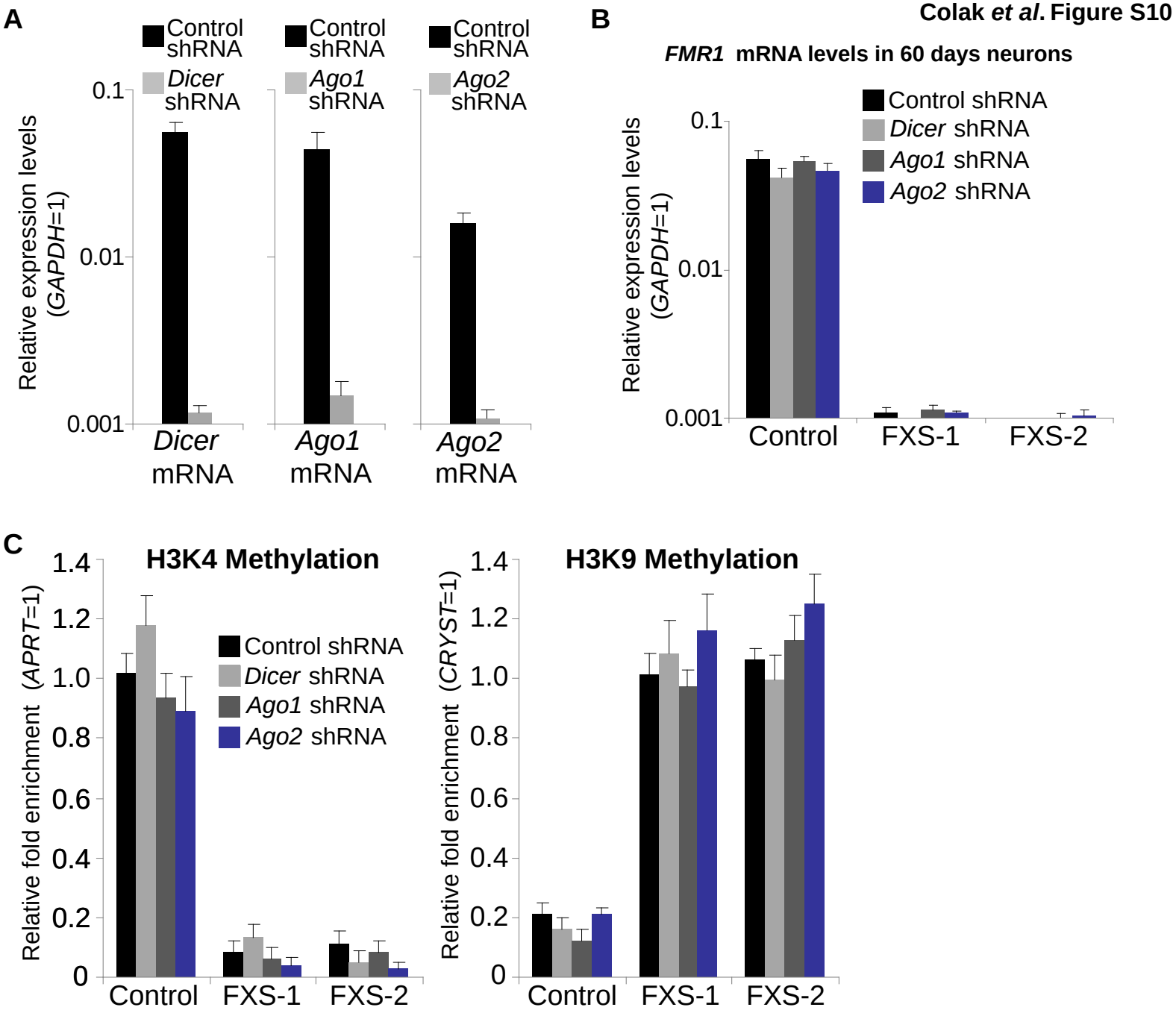
A
Control shRNA
Dicer shRNA
Ago1 shRNA
Ago2 shRNA
Relative expression levels (GAPDH=1)
0.1
0.01
0.001
Dicer mRNA
Ago1 mRNA
Ago2 mRNA
B
FMR1 mRNA levels in 60 days neurons
Control shRNA
Dicer shRNA
Ago1 shRNA
Ago2 shRNA
Relative expression levels (GAPDH=1)
0.1
0.01
0.001
Control
FXS-1
FXS-2
C
H3K4 Methylation
Relative fold enrichment (APRT=1)
1.4
1.2
1.0
0.8
0.6
0.4
0.2
0
Control shRNA
Dicer shRNA
Ago1 shRNA
Ago2 shRNA
Control
FXS-1
FXS-2
H3K9 Methylation
Relative fold enrichment (CRYST=1)
Control
FXS-1
FXS-2

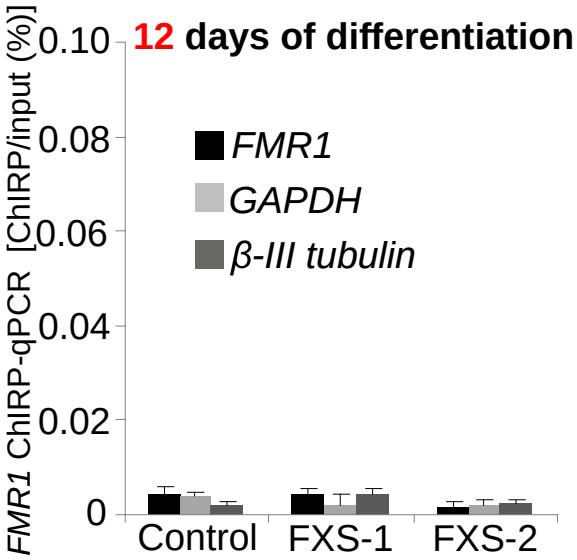
12 days of differentiation
FMR1 ChIRP-qPCR [ChIRP/input (%)]
0.10
0.08
0.06
0.04
0.02
0
FMR1
GAPDH
β-III tubulin
Control
FXS-1
FXS-2

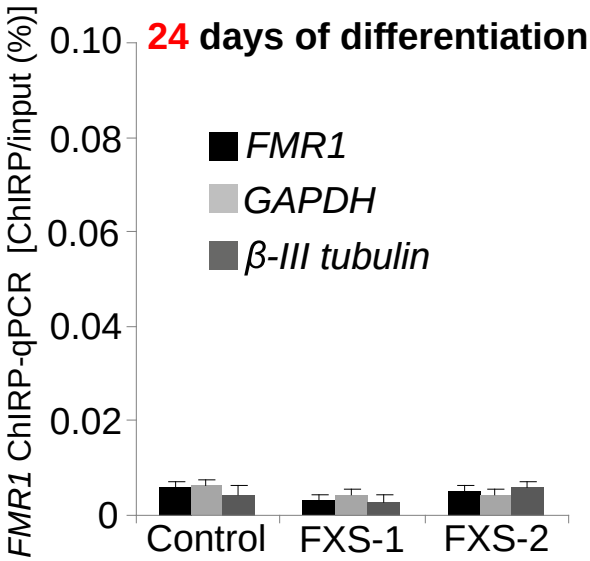
24 days of differentiation
FMR1 ChIRP-qPCR [ChIRP/input (%)]
0.10
0.08
0.06
0.04
0.02
0
FMR1
GAPDH
β-III tubulin
Control
FXS-1
FXS-2

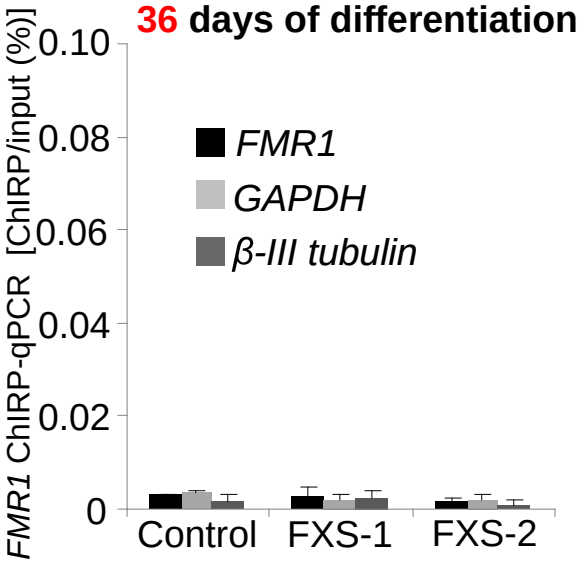
36 days of differentiation
FMR1 ChIRP-qPCR [ChIRP/input (%)]
0.10
0.08
0.06
0.04
0.02
0
FMR1
GAPDH
β-III tubulin
Control
FXS-1
FXS-2

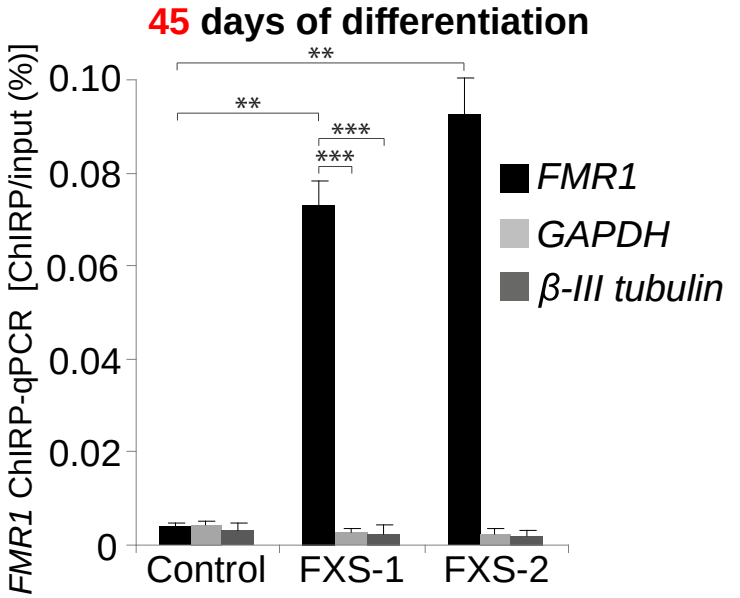
45 days of differentiation
FMR1 ChIRP-qPCR [ChIRP/input (%)]
0.10
0.08
0.06
0.04
0.02
0
**
**
***
***
FMR1
GAPDH
β-III tubulin
Control
FXS-1
FXS-2

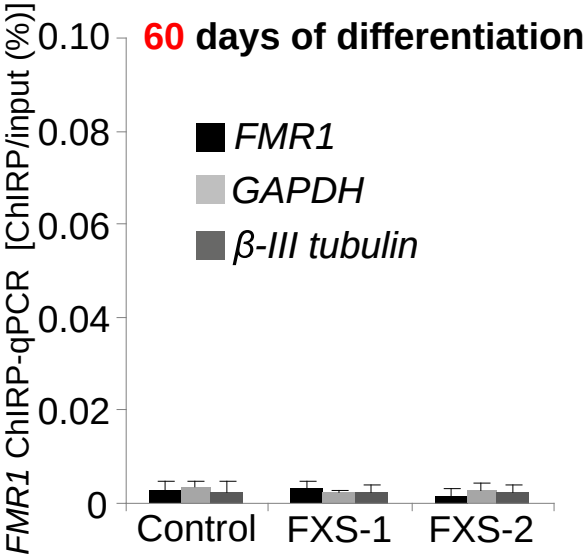
60 days of differentiation
FMR1 ChIRP-qPCR [ChIRP/input (%)]
0.10
0.08
0.06
0.04
0.02
0
FMR1
GAPDH
β-III tubulin
Control
FXS-1
FXS-2

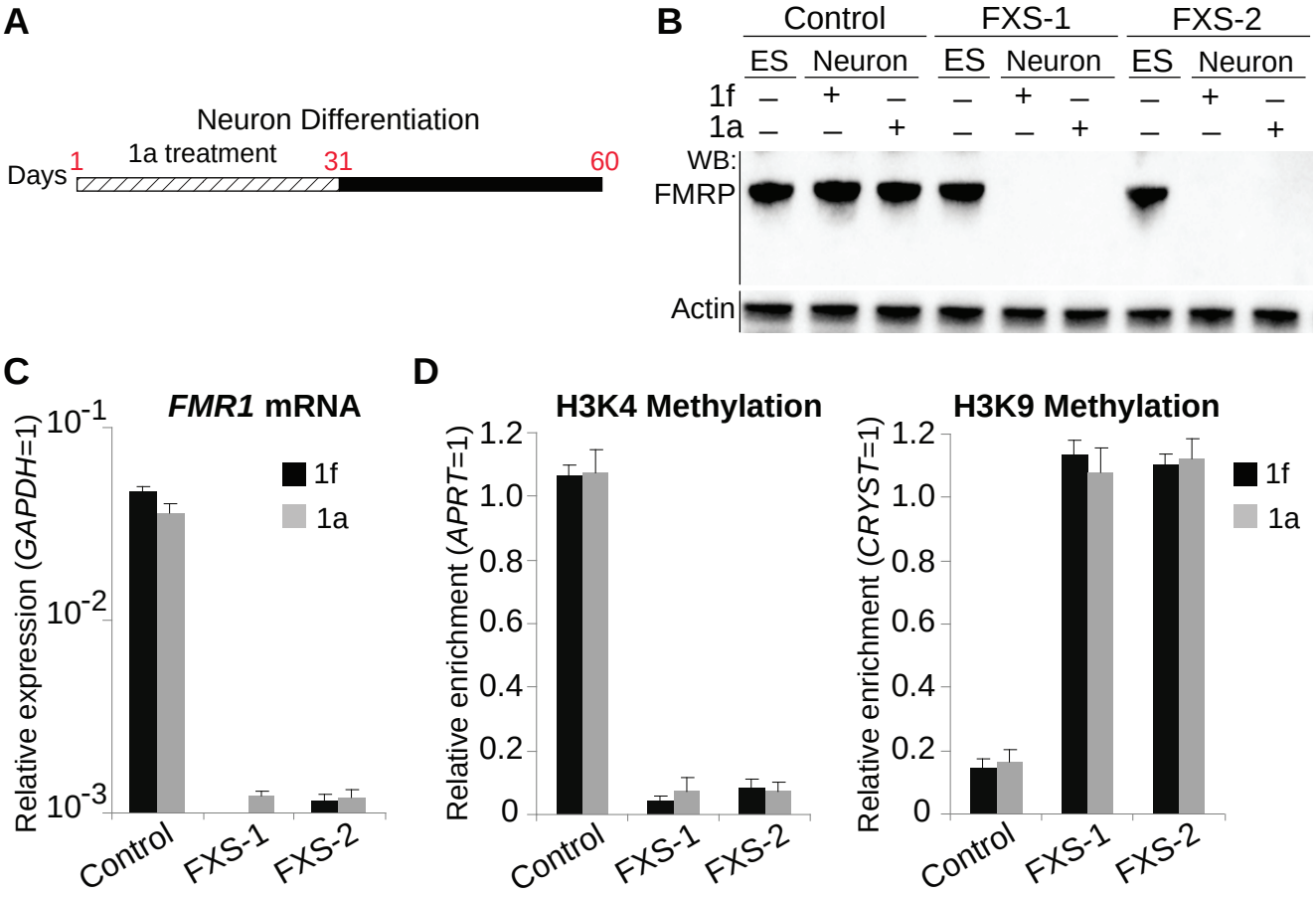
A
Neuron Differentiation
Days
1
1a treatment
31
60
B
Control
FXS-1
FXS-2
ES
Neuron
1f
1a
WB:
FMRP
Actin
C
FMR1 mRNA
Relative expression (*GAPDH*=1)
1f
1a
Control
FXS-1
FXS-2
D
H3K4 Methylation
Relative enrichment (*APRT*=1)
H3K9 Methylation
Relative enrichment (*CRYST*=1)

FMR1 mRNA knockdown during days 31-60 of neuronal differentiation

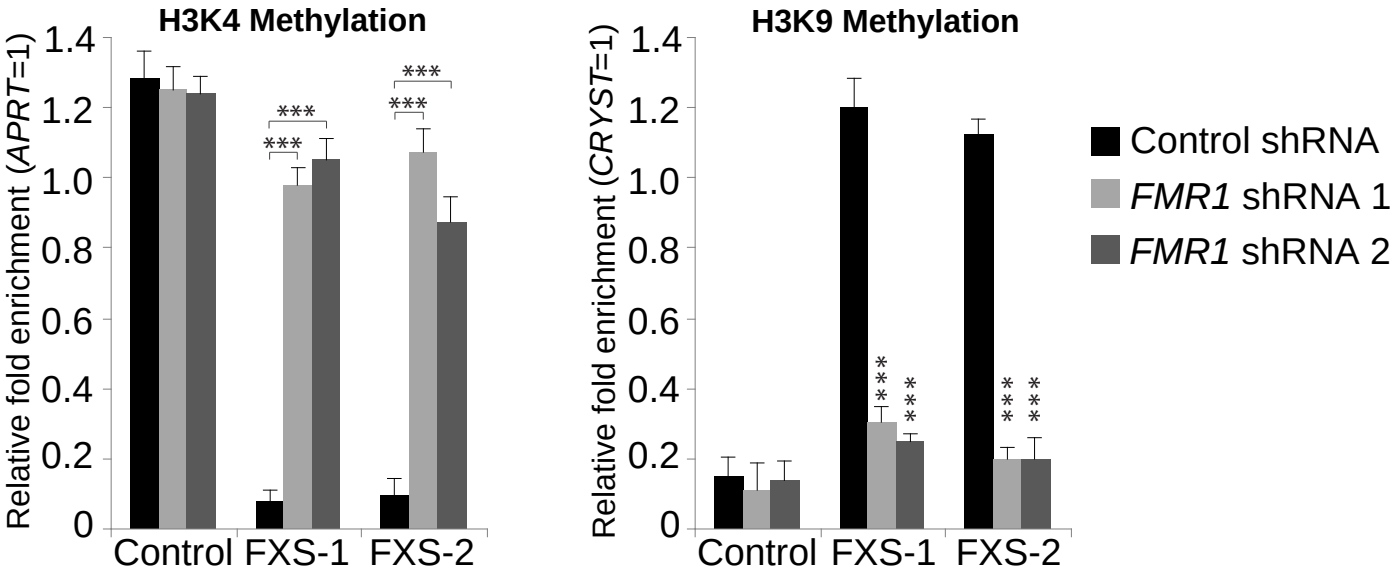

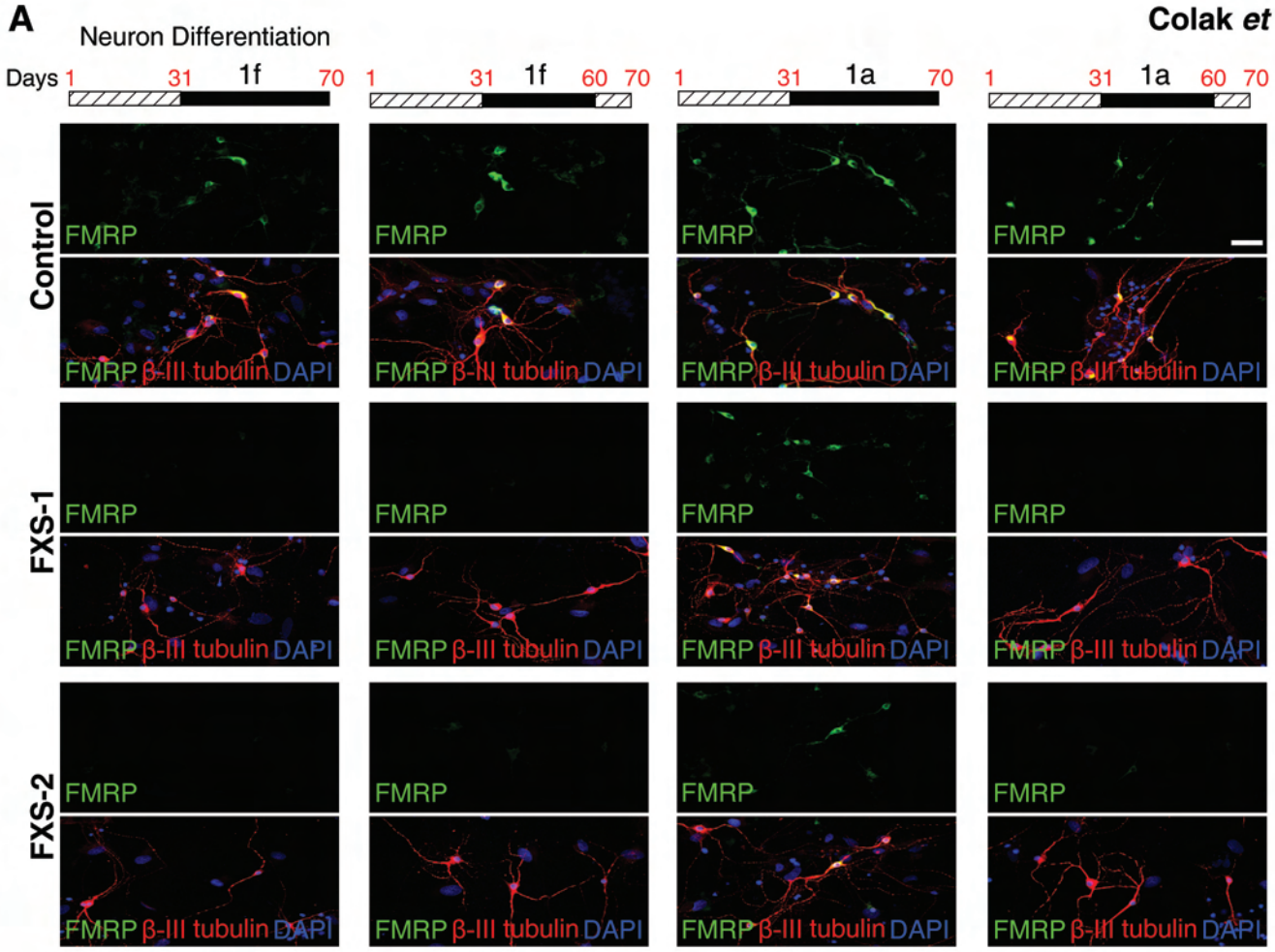
A
Neuron Differentiation
Days 1 31 1f 70
1 31 1f 60 70
1 31 1a 70
1 31 1a 60 70
Control
FXS-1
FXS-2
FMRP
FMRP β-III tubulin DAPI

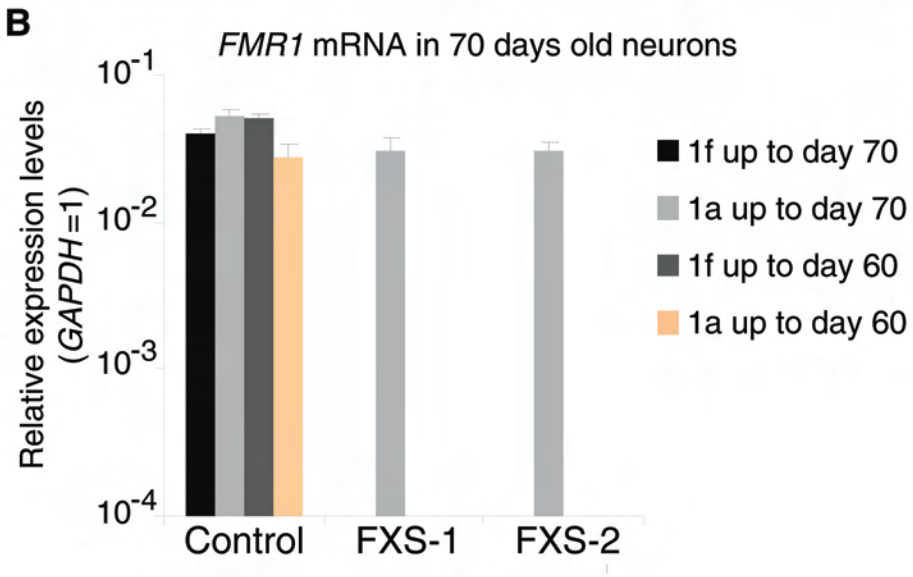
B
FMR1 mRNA in 70 days old neurons
Relative expression levels (*GAPDH*=1)
10^{-1}
10^{-2}
10^{-3}
10^{-4}
Control
FXS-1
FXS-2
1f up to day 70
1a up to day 70
1f up to day 60
1a up to day 60

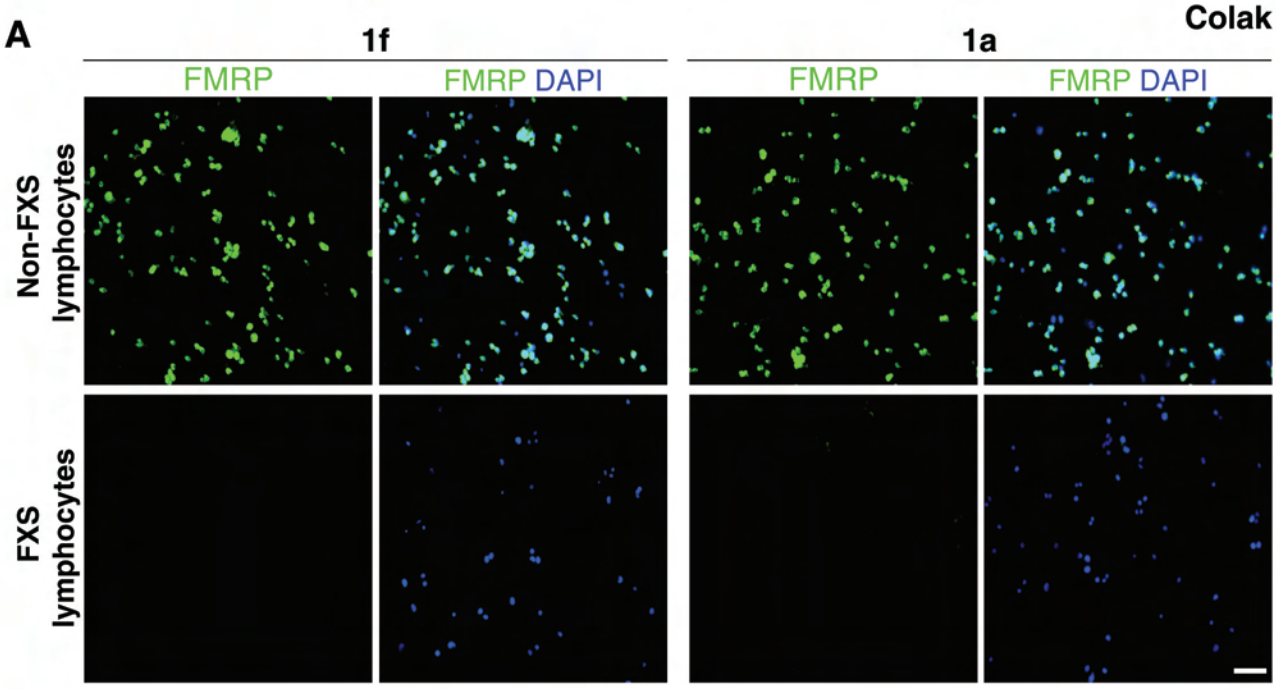
A
1f
1a
FMRP
FMRP DAPI
FMRP
FMRP DAPI
Non-FXS lymphocytes
FXS lymphocytes

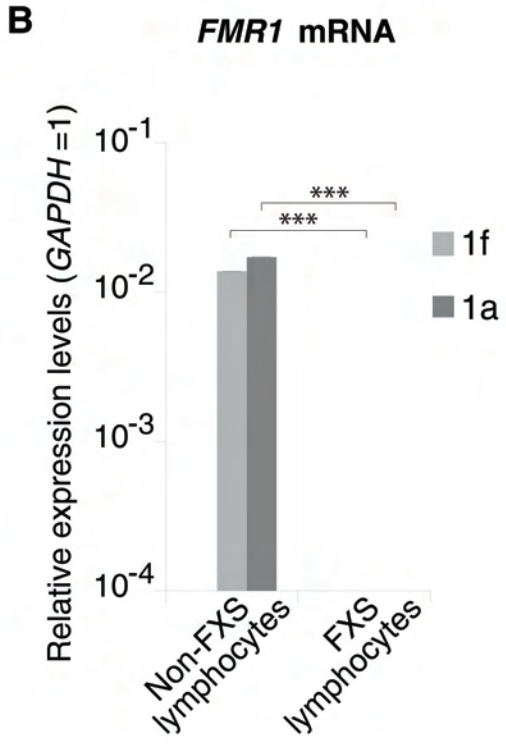
B
FMR1 mRNA
Relative expression levels (*GAPDH*=1)
10^{-1}
10^{-2}
10^{-3}
10^{-4}
***
***
1f
1a
Non-FXS lymphocytes
FXS lymphocytes

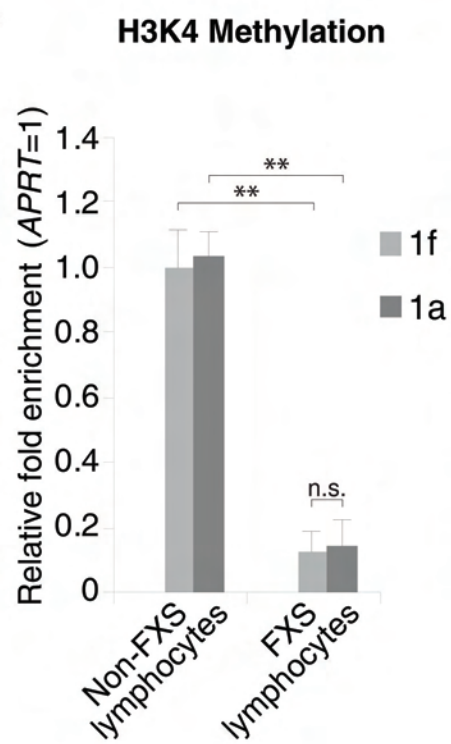
C
H3K4 Methylation
Relative fold enrichment (*APRT*=1)
1.4
1.2
1.0
0.8
0.6
0.4
0.2
0
**
**
n.s.
1f
1a
Non-FXS lymphocytes
FXS lymphocytes

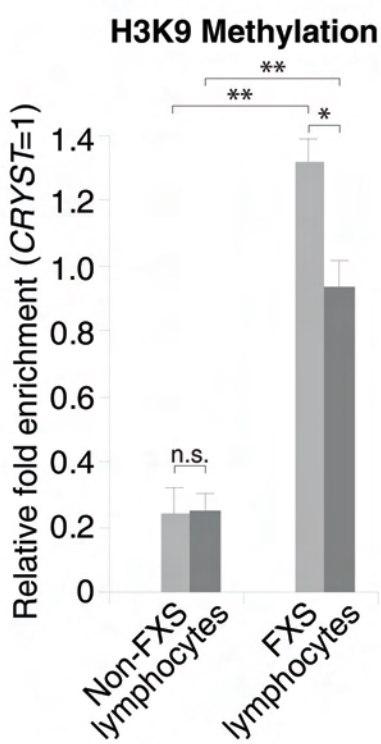
H3K9 Methylation
Relative fold enrichment (*CRYST*=1)
1.4
1.2
1.0
0.8
0.6
0.4
0.2
0
**
**
*
n.s.
Non-FXS lymphocytes
FXS lymphocytes

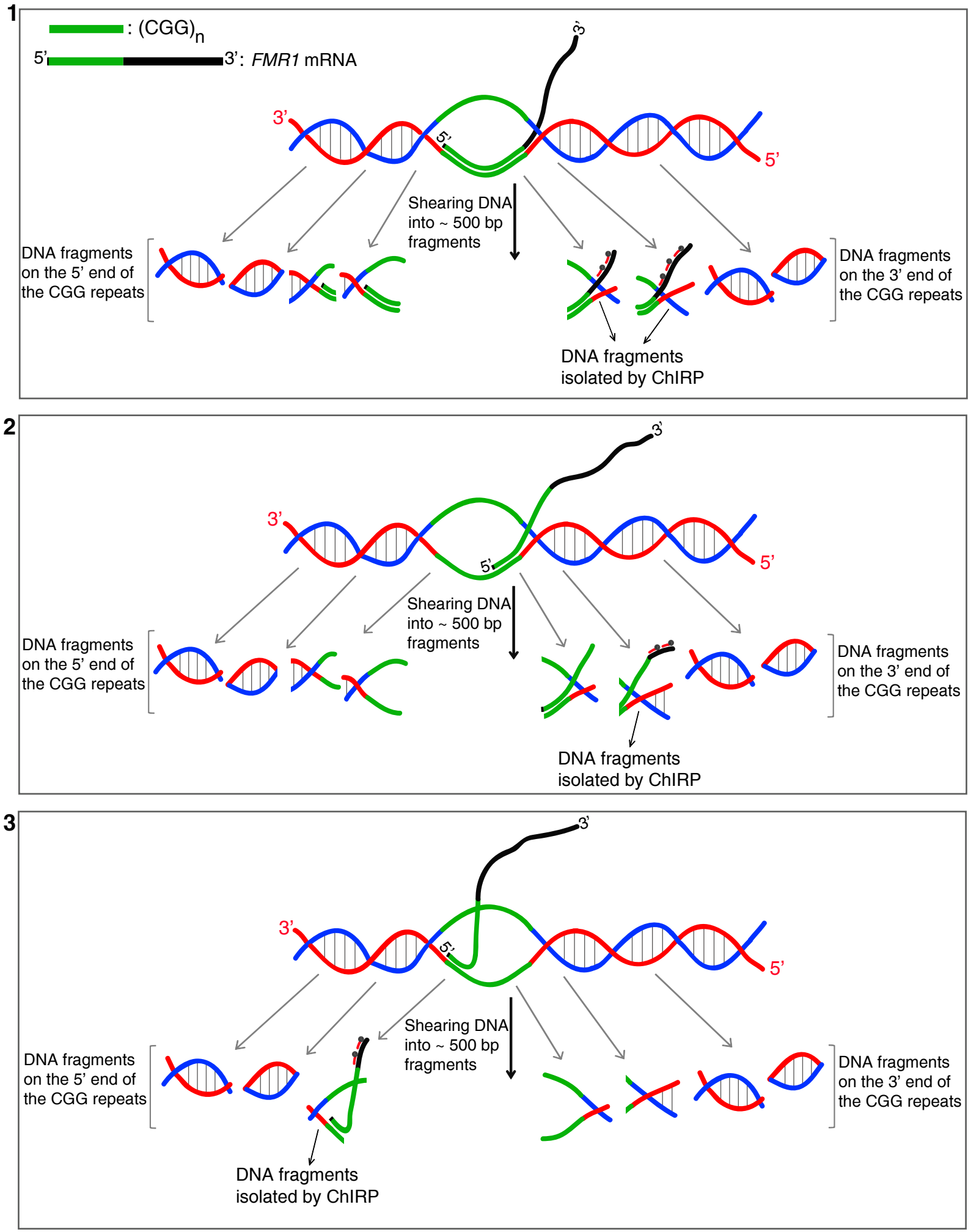
1
: (CGG)n
5'
3': FMR1 mRNA
3'
3'
5'
5'
Shearing DNA into ~ 500 bp fragments
DNA fragments on the 5' end of the CGG repeats
DNA fragments on the 3' end of the CGG repeats
DNA fragments isolated by ChIRP
2
3'
3'
5'
5'
Shearing DNA into ~ 500 bp fragments
DNA fragments on the 5' end of the CGG repeats
DNA fragments on the 3' end of the CGG repeats
DNA fragments isolated by ChIRP
3
3'
3'
5'
5'
Shearing DNA into ~ 500 bp fragments
DNA fragments on the 5' end of the CGG repeats
DNA fragments on the 3' end of the CGG repeats
DNA fragments isolated by ChIRP

Table S1

Probe	Sequence (5' to 3')	
FMR1 _1	cttgtagaaagcgccattgg	
FMR1 _2	gtgggaatctgacatcatga	Probe Set 1
FMR1 _3	tgtaagttgcatcacatgct	
FMR1 _4	cgtaagtcttctggcacatc	
FMR1 _5	tcaatcagcatatgtgctcg	
FMR1 _6	tgttcatgaaatctcgaggc	
FMR1 _7	atgtgcaggtatcttcatct	Probe Set 2
FMR1 _8	ttgcctactaagttccttgg	
FMR1 _9	ctgctacaactgatgaagcc	
FMR1 _10	tccaaaagaacagtggcatt	
FMR1 _11	tggtggtctagaactagctc	
FMR1 _12	gaccaatcactgagttcgtc	Probe Set 3
FMR1 _13	agtgatcgtcgtttcctttg	
FMR1 _14	gtgtggacactcctttcatt	
FMR1 _15	ttagggtactccattcacga	
FMR1 _16	ttgtgttcatttcatgccct	
FMR1 _17	ctggtgaatgatcacccaat	Probe Set 4
FMR1 _18	acacaggacatgaaatgaca	
FMR1 _19	aggcacagatcatacaactt	
FMR1 _20	ttgacagggtttgctacatc	
FMR1 _21	aagagcaggcatatcctact	
FMR1 _22	agtacctgtactttgcagga	Probe Set 5
FMR1 _23	catcagaggcagaacttcag	
FMR1 _24	atcctactaactttcgacca	
FMR1 _25	cctgtactttgcaggattat	

Probe	Sequence (5' to 3')
TERC _1	aggcccaccctccgcaaccc
TERC _2	aaaaatggccaccacccctc
TERC _3	ggcgcctacgcccttctcaa
TERC _4	acagcgcgcggggagcaaaa
TERC _5	ccgctgaaagtcagcgagaa
TERC _6	cggcaggccgaggcttttcc
TERC _7	ctctagaatgaacggtggaa
TERC _8	ccagcagctgacatttttg
TERC _9	aggtccccgggaggggcgaa
TERC _10	ttcgggggctgggcaggcga
TERC _11	cgaccgcggcctccaggcgg
TERC _12	tgcctccggagaagccccgg
TERC _13	aactcttcgcggtggcagtg
TERC _14	agacccgcggctgacagagc
TERC _15	tgaacctcgccctcgccccc
TERC _16	tcttcctgcggcctgaaagg
TERC _17	gcgcggggactcgctccgtt
TERC _18	tcccacagctcagggaatcg
TERC _19	tgagccgagtcctgggtgca

Table S2

Primer	Sequence (5' to 3')	
FMR1 F	gaacagcgttgatcacgtga	TSS - (-200)
FMR1 R	accggaagtgaaaccgaaac	
FMR1 F	agaaatgggcgttctggc	-200 - (-400)
FMR1 R	tctctcttcaagtggcct	
FMR1 F	atccttcacccctattctcg	-400 - (-600)
FMR1 R	atgcatccggttatcccagt	
FMR1 F	atccatgtcccttaaagggc	-600 - (-800)
FMR1 R	cgagaataggggtgaaggat	
FMR1 F	cacatacagtaggggcagaa	-800 - (-1000)
FMR1 R	gccctttaagggacatggat	
FMR1 F	gcagctataagcacggtgta	-1000 - (-1200)
FMR1 R	ttctgcccctactgtatgtg	
FMR1 F	tagcagggctgaagagaaga	ATG - (+200)
FMR1 R	cctgccctagagccaagtac	
FMR1 F	gtacttggctctagggcagg	+200 - (+400)
FMR1 R	ggtctctcatttcgataggc	
FMR1 F	agcgaggagagggttctctt	+400 - (+600)
FMR1 R	ccacaactacccacacgaca	
FMR1 F	tgtcgtgtgggtagttgtgg	+600 - (+800)
FMR1 R	agccactaaaaatcagttgcc	
FMR1 F	ggcaactgatttttagtggct	+800 - (+1000)
FMR1 R	agtagcagcgctgctaatgg	
FMR1 F	ccattagcagcgctgctact	+1000 - (+1200)
FMR1 R	agcctcaacaattcagtcc	

Primer	Sequence (5' to 3')
APRT F	gccttgactcgcacttttgt
APRT R	taggcgccatcgattttaag
CRYSTALLIN F	ccgtggtaccaaagctga
CRYSTALLIN R	agccggctggggtagaag
GAPDH F	aggtttccaggagtgccttt
GAPDH R	acctgataattagggcagac
β-III Tub F	aagctccattcttcccagga
β-III Tub R	ctcaggtccccaggacattt
c-Myc F	cgtctagcacctttgatttctccc
c-Myc R	ctctgccagtctgtaccccaccgt
Cyclin D1 F	cgctcccattctctgccggg
Cyclin D1 R	ccgcgctccctcgcgctctt

Table S3

Primer	Sequence (5' to 3')
S100B F	agctgaagaaatccgaactg
S100B R	acaaaggccatgaattcctg
SYP F	tttgtgaaggtgctgcaatg
SYP R	agacaggcatctccttgata
NeuN F	gatcatttttaacgagcggg
NeuN R	ctcaattttccgtccctcta
MAP2 F	ccaaagagaatgggatcaac
MAP2 R	gtctggtctttatgttgagc
ASIC2 F	agccaagtaccttgagaaga
ASIC2 R	ctagcaccaatgaacaatcc
MAP1B F	aatccgatcatgggacacaa
MAP1B R	tgctgactgcttcatcagaa
TAU F	gagttcgaagtgatggaaga
TAU R	cttagcatcagaggtttcag
UNC13B F	cacatatgtgaccctgaaag
UNC13B R	cgactgacgaatagtcttca
GABRD F	atgaatgacatcggcgacta
GABRD R	tcatggtgtactccatgttg
PPP1R9B F	gctaattcagcagactttgg
PPP1R9B R	ttctccgctagctcaaaca

References

1. A. J. Verkerk, M. Pieretti, J. S. Sutcliffe, Y.-H. Fu, D. P. A. Kuhl, A. Pizzuti, O. Reiner, S. Richards, M. F. Victoria, F. Zhang, B. E. Eussen, G.-J. B. van Ommen, L. A. J. Blonden, G. J. Riggins, J. L. Chastain, C. B. Kunst, H. Galjaard, C. Thomas Caskey, D. L. Nelson, B. A. Oostra, S. T. Warren, Identification of a gene (*FMR-1*) containing a CGG repeat coincident with a breakpoint cluster region exhibiting length variation in fragile X syndrome. *Cell* **65**, 905–914 (1991). doi:10.1016/0092-8674(91)90397-H Medline

2. I. Oberlé, F. Rousseau, D. Heitz, C. Kretz, D. Devys, A. Hanauer, J. Boué, M. F. Bertheas, J. L. Mandel, Instability of a 550-base pair DNA segment and abnormal methylation in fragile X syndrome. *Science* **252**, 1097–1102 (1991). doi:10.1126/science.252.5009.1097 Medline

3. B. Coffee, F. Zhang, S. Ceman, S. T. Warren, D. Reines, Histone modifications depict an aberrantly heterochromatinized *FMR1* gene in fragile x syndrome. *Am. J. Hum. Genet.* **71**, 923–932 (2002). doi:10.1086/342931 Medline

4. R. Willemsen, C. J. Bontekoe, L. A. Severijnen, B. A. Oostra, Timing of the absence of FMR1 expression in full mutation chorionic villi. *Hum. Genet.* **110**, 601–605 (2002). doi:10.1007/s00439-002-0723-5 Medline

5. J. R. Brouwer, E. J. Mientjes, C. E. Bakker, I. M. Nieuwenhuizen, L. A. Severijnen, H. C. Van der Linde, D. L. Nelson, B. A. Oostra, R. Willemsen, Elevated Fmr1 mRNA levels and reduced protein expression in a mouse model with an unmethylated Fragile X full mutation. *Exp. Cell Res.* **313**, 244–253 (2007). doi:10.1016/j.yexcr.2006.10.002 Medline

6. G. Sandberg, M. Schalling, Effect of in vitro promoter methylation and CGG repeat expansion on FMR-1 expression. *Nucleic Acids Res.* **25**, 2883–2887 (1997). doi:10.1093/nar/25.14.2883 Medline

7. R. Eiges, A. Urbach, M. Malcov, T. Frumkin, T. Schwartz, A. Amit, Y. Yaron, A. Eden, O. Yanuka, N. Benvenisty, D. Ben-Yosef, Developmental study of fragile X syndrome using human embryonic stem cells derived from preimplantation genetically diagnosed embryos. *Cell Stem Cell* **1**, 568–577 (2007). doi:10.1016/j.stem.2007.09.001 Medline

8. J. Gerhardt, M. J. Tomishima, N. Zaninovic, D. Colak, Z. Yan, Q. Zhan, Z. Rosenwaks, S. R. Jaffrey, C. L. Schildkraut, The DNA replication program is altered at the FMR1 locus in fragile x embryonic stem cells. *Mol. Cell* **53**, 19–31 (2014). doi:10.1016/j.molcel.2013.10.029 Medline

9. Y. Verlinsky, N. Strelchenko, V. Kukharenko, S. Rechitsky, O. Verlinsky, V. Galat, A. Kuliev, Human embryonic stem cell lines with genetic disorders. *Reprod. Biomed. Online* **10**, 105–110 (2005). doi:10.1016/S1472-6483(10)60810-3 Medline

10. K. Usdin, K. J. Woodford, CGG repeats associated with DNA instability and chromosome fragility form structures that block DNA synthesis in vitro. *Nucleic Acids Res.* **23**, 4202–4209 (1995). doi:10.1093/nar/23.20.4202 Medline

11. P. D. Ladd, L. E. Smith, N. A. Rabaia, J. M. Moore, S. A. Georges, R. S. Hansen, R. J. Hagerman, F. Tassone, S. J. Tapscott, G. N. Filippova, An antisense transcript spanning the CGG repeat region of FMR1 is upregulated in premutation carriers but silenced in full

mutation individuals. *Hum. Mol. Genet.* **16**, 3174–3187 (2007). doi:10.1093/hmg/ddm293 Medline

12. M. D. Disney, B. Liu, W. Y. Yang, C. Sellier, T. Tran, N. Charlet-Berguerand, J. L. Childs-Disney, A small molecule that targets r(CGG)(exp) and improves defects in fragile X-associated tremor ataxia syndrome. *ACS Chem. Biol.* **7**, 1711–1718 (2012). doi:10.1021/cb300135h Medline

13. V. Handa, T. Saha, K. Usdin, The fragile X syndrome repeats form RNA hairpins that do not activate the interferon-inducible protein kinase, PKR, but are cut by Dicer. *Nucleic Acids Res.* **31**, 6243–6248 (2003). doi:10.1093/nar/gkg818 Medline

14. P. Jin, R. S. Alisch, S. T. Warren, RNA and microRNAs in fragile X mental retardation. *Nat. Cell Biol.* **6**, 1048–1053 (2004). doi:10.1038/ncb1104-1048 Medline

15. C. Chu, K. Qu, F. L. Zhong, S. E. Artandi, H. Y. Chang, Genomic maps of long noncoding RNA occupancy reveal principles of RNA-chromatin interactions. *Mol. Cell* **44**, 667–678 (2011). doi:10.1016/j.molcel.2011.08.027 Medline

16. M. D. Simon, C. I. Wang, P. V. Kharchenko, J. A. West, B. A. Chapman, A. A. Alekseyenko, M. L. Borowsky, M. I. Kuroda, R. E. Kingston, The genomic binding sites of a noncoding RNA. *Proc. Natl. Acad. Sci. U.S.A.* **108**, 20497–20502 (2011). doi:10.1073/pnas.1113536108 Medline

17. Y. Feng, L. Lakkis, D. Devys, S. T. Warren, Quantitative comparison of *FMR1* gene expression in normal and premutation alleles. *Am. J. Hum. Genet.* **56**, 106–113 (1995). Medline

18. J. T. Lee, Epigenetic regulation by long noncoding RNAs. *Science* **338**, 1435–1439 (2012). doi:10.1126/science.1231776 Medline

19. B. P. Belotserkovskii, R. Liu, S. Tornaletti, M. M. Krasilnikova, S. M. Mirkin, P. C. Hanawalt, Mechanisms and implications of transcription blockage by guanine-rich DNA sequences. *Proc. Natl. Acad. Sci. U.S.A.* **107**, 12816–12821 (2010). doi:10.1073/pnas.1007580107 Medline

20. E. Grabczyk, M. C. Fishman, A long purine-pyrimidine homopolymer acts as a transcriptional diode. *J. Biol. Chem.* **270**, 1791–1797 (1995). doi:10.1074/jbc.270.4.1791 Medline

21. M. L. Bochman, K. Paeschke, V. A. Zakian, DNA secondary structures: Stability and function of G-quadruplex structures. *Nat. Rev. Genet.* **13**, 770–780 (2012). doi:10.1038/nrg3296 Medline

22. S. G. Mackintosh, K. D. Raney, DNA unwinding and protein displacement by superfamily 1 and superfamily 2 helicases. *Nucleic Acids Res.* **34**, 4154–4159 (2006). doi:10.1093/nar/gkl501 Medline

23. J. Q. Wu, L. Habegger, P. Noisa, A. Szekely, C. Qiu, S. Hutchison, D. Raha, M. Egholm, H. Lin, S. Weissman, W. Cui, M. Gerstein, M. Snyder, Dynamic transcriptomes during neural differentiation of human embryonic stem cells revealed by short, long, and paired-end sequencing. *Proc. Natl. Acad. Sci. U.S.A.* **107**, 5254–5259 (2010). doi:10.1073/pnas.0914114107 Medline

24. S. Guil, M. Esteller, Cis-acting noncoding RNAs: Friends and foes. *Nat. Struct. Mol. Biol.* **19**, 1068–1075 (2012). doi:10.1038/nsmb.2428 Medline

25. R. S. Alisch, T. Wang, P. Chopra, J. Visootsak, K. N. Conneely, S. T. Warren, Genome-wide analysis validates aberrant methylation in fragile X syndrome is specific to the *FMR1* locus. *BMC Med. Genet.* **14**, 18 (2013). doi:10.1186/1471-2350-14-18 Medline

26. M. V. Evans-Galea, A. J. Hannan, N. Carrodus, M. B. Delatycki, R. Saffery, Epigenetic modifications in trinucleotide repeat diseases. *Trends Mol. Med.* **19**, 655–663 (2013). doi:10.1016/j.molmed.2013.07.007 Medline

27. Z. Xi, L. Zinman, D. Moreno, J. Schymick, Y. Liang, C. Sato, Y. Zheng, M. Ghani, S. Dib, J. Keith, J. Robertson, E. Rogaeva, Hypermethylation of the CpG island near the G4C2 repeat in ALS with a C9orf72 expansion. *Am. J. Hum. Genet.* **92**, 981–989 (2013). doi:10.1016/j.ajhg.2013.04.017 Medline

28. J. A. Thomson, J. Itskovitz-Eldor, S. S. Shapiro, M. A. Waknitz, J. J. Swiergiel, V. S. Marshall, J. M. Jones, Embryonic stem cell lines derived from human blastocysts. *Science* **282**, 1145–1147 (1998). doi:10.1126/science.282.5391.1145 Medline

29. S. M. Chambers, C. A. Fasano, E. P. Papapetrou, M. Tomishima, M. Sadelain, L. Studer, Highly efficient neural conversion of human ES and iPS cells by dual inhibition of SMAD signaling. *Nat. Biotechnol.* **27**, 275–280 (2009). doi:10.1038/nbt.1529 Medline

30. C. Chu, J. Quinn, H. Y. Chang, Chromatin isolation by RNA purification (ChIRP). *J. Vis. Exp.* **2012**, 3912 (2012). Medline

31. M. Telias, M. Segal, D. Ben-Yosef, Neural differentiation of Fragile X human embryonic stem cells reveals abnormal patterns of development despite successful neurogenesis. *Dev. Biol.* **374**, 32–45 (2013). doi:10.1016/j.ydbio.2012.11.031 Medline

32. D. C. Bittel, N. Kibiryeva, M. G. Butler, Whole genome microarray analysis of gene expression in subjects with fragile X syndrome. *Genet. Med.* **9**, 464–472 (2007). doi:10.1097/GIM.0b013e3180ca9a9a Medline

33. M. Qin, K. C. Schmidt, A. J. Zametkin, S. Bishu, L. M. Horowitz, T. V. Burlin, Z. Xia, T. Huang, Z. M. Quezado, C. B. Smith, Altered cerebral protein synthesis in fragile X syndrome: Studies in human subjects and knockout mice. *J. Cereb. Blood Flow Metab.* **33**, 499–507 (2013). doi:10.1038/jcbfm.2012.205 Medline

34. F. A. Buske, J. S. Mattick, T. L. Bailey, Potential in vivo roles of nucleic acid triple-helices. *RNA Biol.* **8**, 427–439 (2011). doi:10.4161/rna.8.3.14999 Medline